Oncogene (2012), 1–15

www.nature.com/onc

ORIGINAL ARTICLE

Annexin A6 is a scaffold for PKCα to promote EGFR inactivation

M Koese[1], C Rentero[2], BP Kota[1], M Hoque[1], R Cairns[1], P Wood[1], S Vilà de Muga[2], M Reverter[2], A Alvarez-Guaita[2], K Monastyrskaya[3], WE Hughes[4], A Swarbrick[4], F Tebar[2], RJ Daly[4], C Enrich[2] and T Grewal[1]

Protein kinase Cα (PKCα) can phosphorylate the epidermal growth factor receptor (EGFR) at threonine 654 (T654) to inhibit EGFR tyrosine phosphorylation (pY-EGFR) and the associated activation of downstream effectors. However, upregulation of PKCα in a large variety of cancers is not associated with EGFR inactivation, and factors determining the potential of PKCα to downregulate EGFR are yet unknown. Here, we show that ectopic expression of annexin A6 (AnxA6), a member of the Ca^{2+} and phospholipid-binding annexins, strongly reduces pY-EGFR levels while augmenting EGFR T654 phosphorylation in EGFR overexpressing A431, head and neck and breast cancer cell lines. Reduced EGFR activation in AnxA6 expressing A431 cells is associated with reduced EGFR internalization and degradation. RNA interference (RNAi)-mediated PKCα knockdown in AnxA6 expressing A431 cells reduces T654-EGFR phosphorylation, but restores EGFR tyrosine phosphorylation, clonogenic growth and EGFR degradation. These findings correlate with AnxA6 interacting with EGFR, and elevated AnxA6 levels promoting PKCα membrane association and interaction with EGFR. Stable expression of the cytosolic N-terminal mutant $AnxA6_{1-175}$, which cannot promote PKCα membrane recruitment, does not increase T654-EGFR phosphorylation or the association of PKCα with EGFR. AnxA6 overexpression does not inhibit tyrosine phosphorylation of the T654A EGFR mutant, which cannot be phosphorylated by PKCα. Most strikingly, stable plasma membrane anchoring of AnxA6 is sufficient to recruit PKCα even in the absence of EGF or Ca^{2+}. In summary, AnxA6 is a new PKCα scaffold to promote PKCα-mediated EGFR inactivation through increased membrane targeting of PKCα and EGFR/PKCα complex formation.

Oncogene advance online publication, 16 July 2012; doi:10.1038/onc.2012.303

Keywords: annexin A6; scaffold; PKCα; EGF receptor

INTRODUCTION

Overexpression or mutation of the epidermal growth factor receptor (EGFR, ErbB1) is common in breast, head and neck, and other cancers, leading to aberrant activation of effector pathways and cell transformation.[1] At the cell surface, ligand binding results in EGFR dimerization and activation of its tyrosine kinase (TK) domain. This triggers EGFR tyrosine autophosphorylation and binding of adapters, which link EGFR to downstream effectors that regulate proliferation and differentiation.[2,3] To avoid constitutive signaling, ligand binding also initiates rapid EGFR internalization and lysosomal degradation.[2,4,5]

Alternatively, heterologous desensitization of EGFR can occur through the protein kinase C (PKC) family of serine/threonine kinases activated by G-protein coupled receptors, platelet-derived growth factor, hormone-induced phosphatidylinositol turnover or tumor-promoting phorbol esters (TPA).[6–10] PKC-mediated phosphorylation of threonine 654 (T654) inhibits EGFR TK activity[6,8,10–12] and consequently, reduces EGFR internalization and lysosomal degradation, as inactive EGFR is diverted to recycling endosomes for transport back to the cell surface.[13,14]

Pharmacological inhibitors with increased PKC isoform specificity, RNAi knockdown and co-immunoprecipitations suggest that the widely expressed PKCα isoform interacts and phosphorylates T654-EGFR in normal colon and intestinal epithelial cells, and also pancreatic and squamous carcinoma.[15,16] Like other PKCs, PKCα is rapidly recruited to the plasma membrane upon activation of phospholipase C, subsequent production of diacylglycerol and elevation of Ca^{2+}.[17] Ca^{2+} binding increases the affinity of PKCα for phosphatidylserine, which is followed by diacylglycerol binding and conformational changes to allow substrate binding and phosphorylation.[18,19] In addition, Receptors for activated C kinase (RACKs) and A-kinase-anchoring protein (AKAP) 79/150 act as compartment- and signal-organizing scaffolds to promote and control phosphorylation of PKC isozyme substrates.[18,20,21] Membrane-bound RACKs and AKAPs selectively bind a particular PKC isozyme only in the active conformation and similar to other scaffolds, their relative amounts and differential expression contribute to signal specificity.[18,21]

Other PKC scaffolds include annexins (Anx), which similar to conventional PKCs, bind to negatively charged phospholipids in a Ca^{2+}-dependent manner.[22–24] AnxA5 shuttles PKCδ from the cytosol to the membrane,[25] while AnxA1 and AnxA2 interact with PKCβ and PKCε, respectively.[26,27] Furthermore, we and others showed that AnxA6 interacts and promotes membrane association of PKCα.[28,29] Like other scaffolds of the EGFR/Ras/mitogen-activated protein kinase (MAPK) pathway,[30–32] AnxA6 binds to various members of this signaling cascade to reduce signal output, including H-Ras and the Ras-GTPase activating protein p120GAP,[33–35] which probably stabilizes p120GAP/H-Ras assembly to inhibit Ras signaling. In addition, AnxA6 interacts with Raf-1[36] and EGFR (Blagoev *et al.*;[37] for reviews, see Grewal and Enrich,[24] Grewal *et al.*[38] and Enrich *et al.*[39]). Downregulation of

[1]Faculty of Pharmacy, University of Sydney, Sydney, New South Wales, Australia; [2]Departament de Biologia Cel·lular, Immunologia i Neurociències, Institut d'Investigacions Biomèdiques August Pi i Sunyer (IDIBAPS), Facultat de Medicina, Universitat de Barcelona, Barcelona, Spain; [3]Department of Clinical Research, Urology Research Laboratory, University of Bern, Bern, Switzerland and [4]Garvan Institute of Medical Research, Darlinghurst, New South Wales, Australia. Correspondence: Professor C Enrich, Departament de Biologia Cel·lular, Facultat de Medicina, Universitat de Barcelona, Casanova 143, 08036 Barcelona, Spain or Dr T Grewal, University of Sydney, Sydney, New South Wales 2006, Australia.
E-mail: enrich@ub.edu or thomas.grewal@sydney.edu.au
Received 11 August 2011; revised 25 May 2012; accepted 31 May 2012

AnxA6 in EGFR overexpressing A431 epidermoid carcinoma, EGFR overexpressing (BT20, MDA-MB-468) and estrogen receptor (ER)-negative breast cancer cell lines (BCCs)[35] and human breast carcinoma[40] suggest that cell transformation and cancer progression deplete cells of a scaffold that could downregulate oncogenic signaling.

In the absence of heterologous stimuli, PKCα-mediated EGFR T654 phosphorylation does not contribute to negative feedback mechanisms downregulating EGFR in cell culture models.[41,42] Little is known if EGFR T654 phosphorylation occurs in cancers and since there is no direct correlation between PKCα levels and EGFR activation in various tumors, including breast cancers, this could suggest that other factors may determine a modulating role for PKCα in EGFR signaling.[43,44] Indeed, in SCC12 human squamous carcinoma cells, CD82, caveolin-1 and ganglioside GM3 are required for PKCα-mediated EGFR T654 phosphosporylation.[16] Alternatively, members of the protein kinase N (PNK) family have recently been shown to contribute to basal, but not EGF-stimulated, T654-EGFR phosphorylation.[45] Here, we demonstrate that AnxA6 is a scaffold for PKCα to promote EGFR T654 phosphorylation upon EGF stimulation, which is associated with reduced EGFR tyrosine phosphorylation, internalization and degradation. PKCα depletion restores EGFR tyrosine phosphorylation and cell growth in AnxA6 expressing A431 cells. AnxA6 levels modulate the ability of PKCα to interact with and downregulate ligand-induced EGFR signaling. AnxA6 interacts with both EGFR and PKCα and increases PKCα membrane association. Most strikingly, stable membrane anchoring of AnxA6 increases PKCα levels at the plasma membrane even in unstimulated cells. Altogether, these findings suggest that elevated AnxA6 levels facilitate PKCα-dependent negative feedback mechanisms to downregulate ligand-induced EGFR signaling.

RESULTS

AnxA6 inhibits EGFR tyrosine phosphorylation

AnxA6 has been co-purified with activated EGFR[37,46] and promotes membrane association of PKCα.[29] To investigate if these observations could be linked to EGFR signaling, we compared EGFR tyrosine phosphorylation in EGFR immunoprecipitates from A431 cells, which express $\sim 1\text{–}3 \times 10^6$ EGF receptors/cell, but lack endogenous AnxA6 (A431wt), and A431 stably expressing AnxA6 (A431-A6),[34,35,47] using an anti-phosphotyrosine-specific antibody (Figure 1A). A431wt and A431-A6 cells express comparable amounts of EGFR, and EGF robustly stimulates EGFR tyrosine phosphorylation (pY-EGFR) in A431wt cells (compare lanes 1 and 2). In contrast, EGF-induced tyrosine phosphorylation of EGFR was reduced by $83 \pm 8\%$ in A431-A6 cells (lanes 3 and 4). Next, we analyzed EGFR activation in A431 cells ± AnxA6 by immunofluorescence microscopy (Figure 1B). EGFR is predominantly localized at the cell surface in both cell lines (Figure 1B, panels a and b) and concentrated in plasma membrane-enriched fractions upon fractionation using Percoll gradients (Supplementary Figure S1a). In unstimulated cells, anti-phosphotyrosine (pY) staining at the cell surface of both cell lines was not detectable (Figure 1B, panels c and d). Consistent with the results from EGFR immunoprecipitates, EGF-stimulated A431wt cells displayed a very strong anti-pY staining at the plasma membrane (Figure 1B, panel e), while anti-pY staining remained almost undetectable in A431-A6 upon EGF stimulation (panel f).

To compare if Ca^{2+} elevation could downregulate pY-EGFR levels in A431wt and A431-A6 cells, A431wt and A431-A6 cells were preincubated ± Ca^{2+}-ionophore for 3 min to elevate cellular Ca^{2+} levels, followed by addition of EGF (10 ng/ml) for 5 min. Then, crude membranes were isolated by ultracentrifugation, and analyzed for the amounts of activated EGFR and Erk1/2 (Figure 1C). In A431wt, EGF stimulates EGFR tyrosine phosphorylation (compare lanes 1 and 2), and Ca^{2+} elevation further increased EGF-inducible pY-EGFR levels (compare lanes 2 and 4). In line with Figures 1A and B, EGF-induced pY-EGFR levels in A431-A6 cells were reduced $62 \pm 10\%$ (Figure 1C, compare lanes 1–2 and 5–6). In contrast to A431wt cells, EGFR tyrosine phosphorylation of EGF-stimulated A431-A6 cells was completely abolished with ionomycin (compare lanes 3–4 and 7–8). Consistent with AnxA6 inhibiting EGFR effector pathways,[34,35] possibly in a Ca^{2+}-dependent manner, Erk1/2 phosphorylation (P-Erk1/2) in A431-A6 cells was reduced ± ionomycin (Figure 1C, compare lanes 1–2 and 5–6, 3–4 and 7–8).

We have previously demonstrated that AnxA6 potentiates the Ca^{2+}-dependent membrane targeting of PKCα in Chinese Hamster Ovary (CHO) cells.[29] Similarly, A431-A6 cells exhibited higher levels of membrane-associated PKCα ± EGF (Figure 1C, compare lanes 1–2 with 5–6) and Ca^{2+} elevation compared with A431wt controls (compare lanes 3–4 with 7–8). The increased ratios of membrane-associated vs cytosolic PKCα in A431-A6 cells ± EGF support these findings (Supplementary Figure S1b). As shown for EGFR overexpressing BCCs stably overexpressing AnxA6,[35] membranes from unstimulated and EGF-treated A431-A6 cells contain significant amounts of AnxA6 (Figure 1C, lanes 5–8; Supplementary Figure S1b). This might reflect substantial amounts of membrane-associated and Ca^{2+}-independent AnxA6 proteins described previously.[48] In addition, another pool of AnxA6 proteins is targeted to the membrane in a Ca^{2+}-dependent manner (Figure 1C, lanes 7 and 8). Taken together, this suggested that AnxA6-induced PKCα membrane association might establish negative feedback loops upon EGF or Ca^{2+} activation that facilitate EGFR inhibition.

Annexin A6 promotes T654 phosphorylation of EGFR

Based on AnxA6 reducing pY-EGFR levels, increasing PKCα membrane association (Figures 1A–C) and interacting with PKCα,[28,29] we hypothesized that AnxA6 might increase T654-EGFR phosphorylation, possibly in an EGF- and PKCα-dependent manner, to inactivate EGFR. In fact, strong PKC stimuli, such as TPA, promote heterologous desensitization of EGFR, even in A431wt cells[6–10,42] and consistent with these studies, TPA strongly inhibited EGF-inducible EGFR tyrosine phosphorylation in both A431wt and A431-A6 cells (Supplementary Figure S1c).

To determine if elevated AnxA6 levels promote EGF-inducible T654-EGFR phosphorylation, EGFR immunoprecipitates from A431wt and A431-A6 cells that were analyzed for pY-EGFR (see Figure 1A), were examined for pT654-EGFR levels and co-precipitation of AnxA6 and PKCα. Similarly to previous studies,[7,41,42] EGF induced minor EGFR T654 phosphorylation in A431wt (Figure 2A, lanes 1 and 2), using an antibody specifically recognizing pT654-EGFR. In contrast, EGF-stimulated A431-A6 cells displayed much stronger phosphorylation of T654-EGFR (lanes 3 and 4). Kinetic studies in EGF-stimulated A431wt cells comparing the profiles of pY- and pT654-EFGR levels ($t = 0\text{–}30$ min) revealed rapid downregulation of EGFR tyrosine phosphorylation, while pT654-EGFR levels remained low throughout the incubation period. In contrast, in A431-A6 cells, T654-EGFR phosphorylation peaked at $t = 5$ min to return to basal levels thereafter (Supplementary Figure S1d). At this time point ($t = 5$ min), we observed increased pT654-EGFR staining at the plasma membrane of EGF-incubated A431-A6 cells (see arrows in Supplementary Figure S1e), indicating that AnxA6-stimulated and PKCα-mediated EGFR inhibition occurs predominantly at the plasma membrane during early stages of EGFR signaling. AnxA6-induced upregulation of pT654-EGFR levels in A431 was not associated with aberrant upregulation of PKCα or others PKC isoforms, as judged

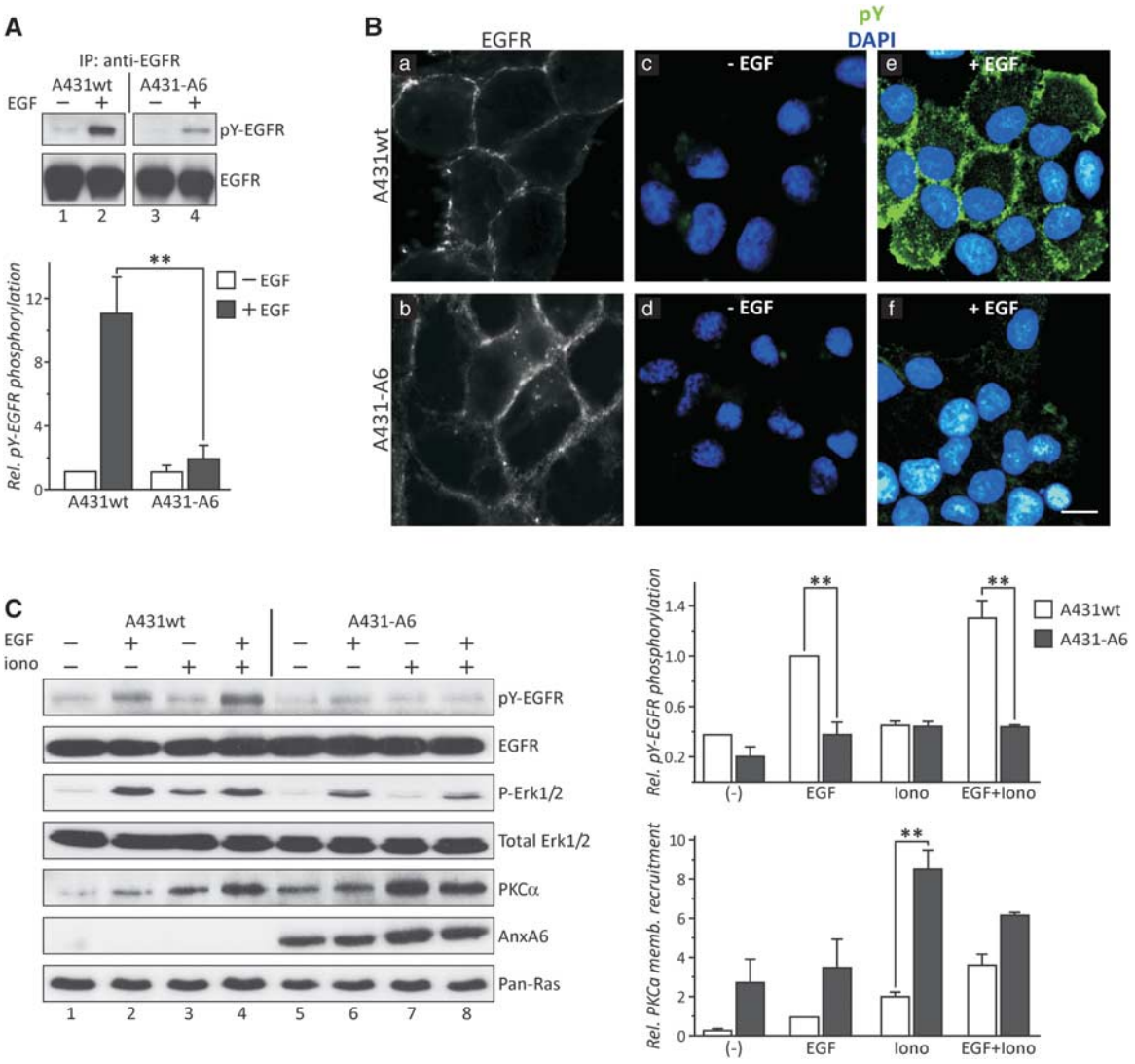

Figure 1. AnxA6 inhibits EGFR activation in EGFR overexpressing cells. (**A**) Cell lysates from A431wt (lanes 1 and 2) and A431-A6 cells (lanes 3 and 4) incubated ± EGF (10 ng/ml for 3 min) were immunoprecipitated with mouse monoclonal anti-EGFR and analyzed for tyrosine phosphorylation (pY-EGFR) and total EGFR by western blotting. Relative levels of activated EGFR in A431wt and A431-A6 from five independent experiments were quantified and normalized to total EGFR. The mean values (± s.e.m.) are shown (**$P < 0.01$ for Student's *t*-test). (**B**) A431wt and A431-A6 cells were plated on coverslips, starved overnight, incubated ± 50 ng/ml EGF for 3 min, fixed and stained with anti-EGFR (EGFR, panels a and b), anti-phosphotyrosine (pY-EGFR) and 4,6-diamidino-2-phenylindole dihydrochloride (panels c–f) as indicated. For comparison of the phosphotyrosine staining intensity in A431wt and A431-A6 cells, experiments were performed in parallel, and images were captured using identical contrast and exposure times. Bar is 10 μm. (**C**) Crude membranes from A431wt (lanes 1–4), A431-A6 (lanes 5–8), preincubated ± ionomycin (2 μM for 3 min), followed by addition of EGF (10 ng/ml for 3 min), were analyzed by western blotting for tyrosine phosphorylated (pY-EGFR) and total EGFR, activated Erk1/2 (P-Erk1/2) and Total Erk1/2, PKCα, AnxA6, and Pan Ras as indicated. Relative levels of activated EGFR and membrane-bound PKCα in A431wt (white bars) and A431-A6 cells (black bars) from three independent experiments were quantified, normalized to total EGFR and Pan Ras, respectively. The mean values (± s.e.m.) are shown (**$P < 0.01$ for Student's *t*-test).

by western blot analysis using PKC isoform-specific antibodies (Supplementary Figure S1f).

Consistent with published data,[16] PKCα co-immunoprecipitated with EGFR in A431wt cells with EGF. Although A431wt and A431-A6 express comparable amounts of PKCα (Supplementary Figures S1b and f), A431-A6 cells displayed increased and EGF-inducible co-immunoprecipitation of PKCα with EGFR (Figure 2A, compare lanes 1–2 with 3–4). Stable expression of the cytosolic N-terminal mutant $AnxA6_{1-175}$, which lacks AnxA6 repeats 3–8, and cannot promote PKCα membrane recruitment,[29] did not stimulate T654-EGFR phosphorylation or association of PKCα with EGFR (Supplementary Figure S1g). Together with AnxA6 co-precipitating with EGFR in an EGF-inducible manner in A431-A6 cells (Figure 2A, lanes 3 and 4), these results indicate that AnxA6/EGFR interaction might increase the association of PKCα with EGFR.

To rule out limiting amounts of activated PKCα in A431wt cells, A431 ± AnxA6 were transfected with constitutively active PKCα (CA-PKCα), starved overnight, incubated ± EGF and cell lysates were subjected to EGFR immunoprecipitations (Figure 2B). In favor of AnxA6 increasing EGFR/PKCα interaction, increased amounts of CA-PKCα co-immunoprecipitated with anti-EGFR in A431-A6 cells ± EGF compared with controls (compare lanes 1–2 with 3–4). As shown above (Figure 2A), increased co-immunoprecipitation of PKCα with EGFR in A431-A6 cells correlated with upregulated basal and EGF-stimulated pT654-EGFR levels (Figure 2B).

To further characterize potential interaction of EGFR and AnxA6 in living cells, COS-1 cells were co-transfected with AnxA6-CFP and EGFR-YFP (yellow fluorescent protein), stimulated ± EGF, fixed and analyzed by confocal microscopy (Figure 2C). In unstimulated cells, AnxA6 is predominantly cytosolic[35,49] and does not colocalize with EGFR (panels a–c, see also enlarged squares).

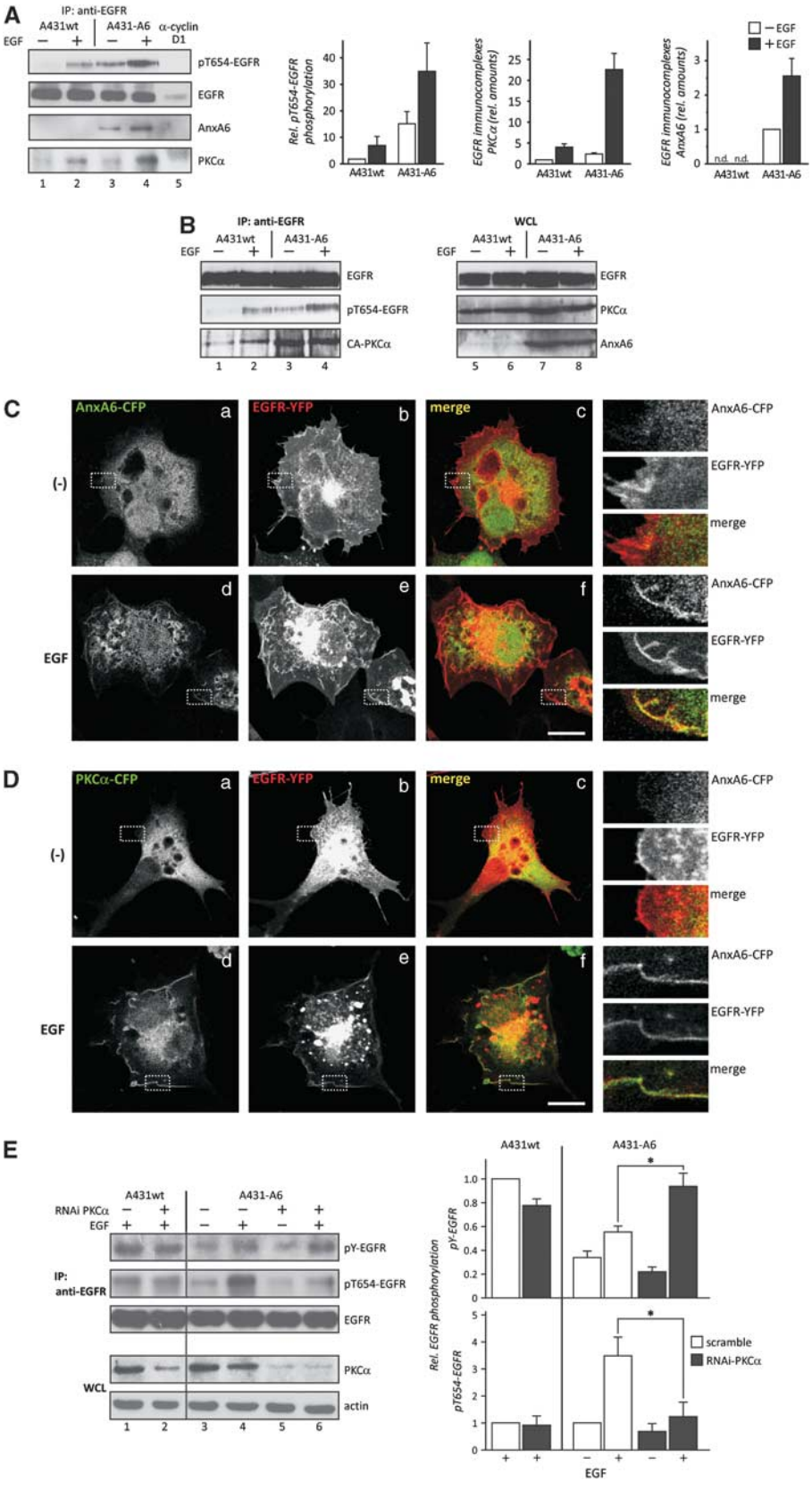

In agreement with the biochemical data (Figures 1 and 2), EGF and Ca^{2+} (not shown) stimulated translocation and colocalization of AnxA6-CFP with EGFR-YFP at the plasma membrane (panels d–f, see arrows in enlarged sections). Interestingly, colocalization of AnxA6 and EGFR appeared more prominent in structures that could resemble circular dorsal ruffles ('waves'), which are dynamic

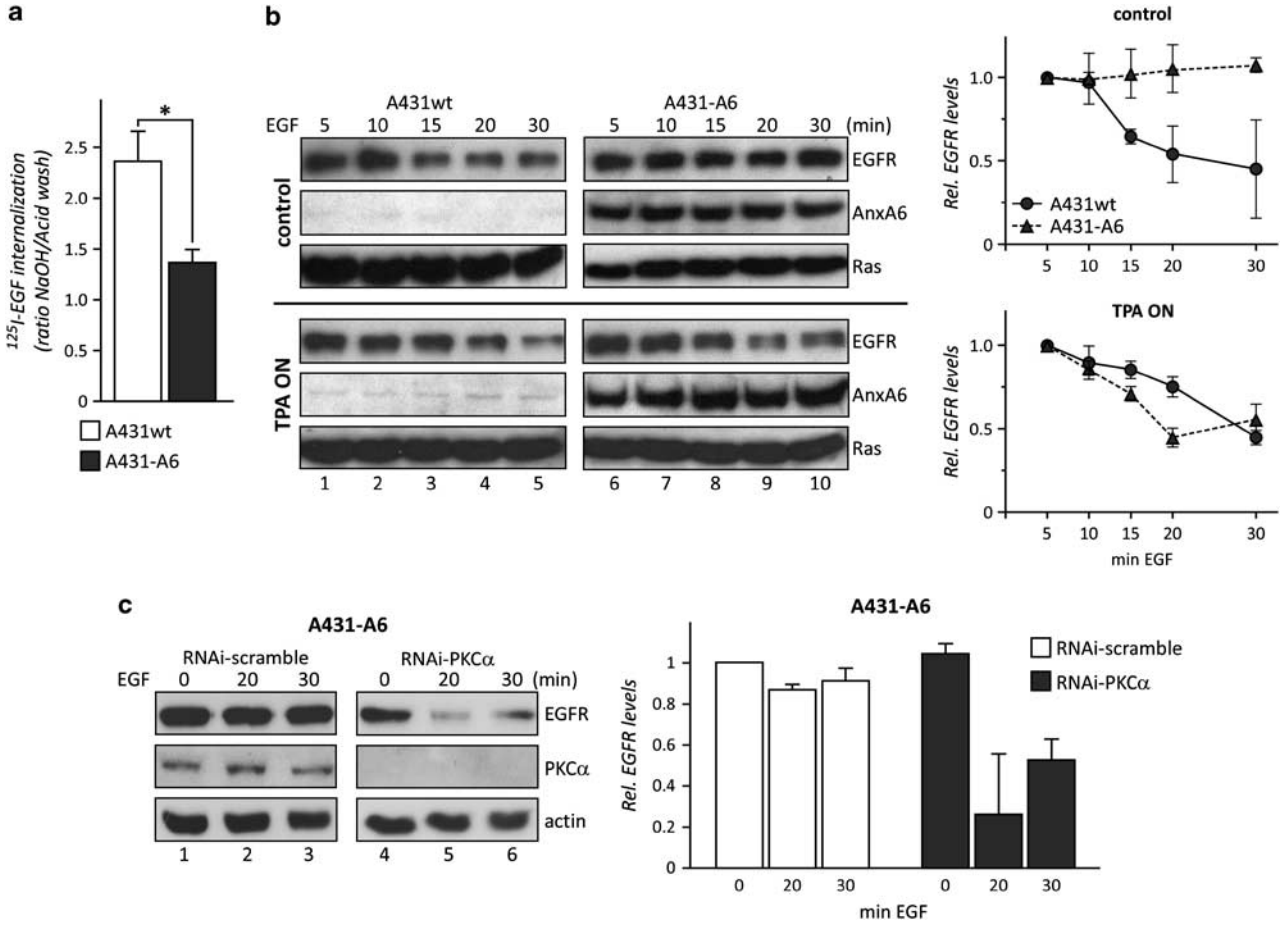

Figure 3. AnxA6 inhibits EGFR internalization and degradation. (**a**) A431wt (white bar) and A431-A6 (black bar) cells were incubated with 5 ng/ml ^{125}I-EGF for 5 min at 37 °C. Non-internalized ^{125}I-EGF was removed, cells were lysed and the amount of internalized ^{125}I-EGF was determined. The ratio of internalized and non-internalized ^{125}I-EGF was calculated and mean values (± s.e.m.) from three independent experiments with triplicate samples are given (*$P < 0.05$ for Student's *t*-test). (**b**) A431wt and A431-A6 cells were preincubated with (TPA ON) or without 500 nM TPA (control) overnight to deplete PKC. Cells were serum starved and incubated with 10 ng/ml EGF for 5, 10, 15, 20 and 30 min as indicated. Cell lysates from each time point were analyzed for the amount of EGFR, AnxA6 and Ras. In two independent experiments, the relative amount of EGFR in each sample was calculated and normalized to Pan-Ras. The mean values (± s.e.m.) are given. (**c**) A431-A6 cells with stable PKCα knockdown were incubated ± 10 ng/ml EGF for 0, 20 and 30 min as indicated. A431-A6 cells stably expressing scrambled RNAi served as negative control. Cell lysates from each time point were analyzed for the amount of EGFR, PKCα and actin. Two different blots for PKCα and EGFR, respectively, were joined together in this presentation. In two independent experiments, the relative amount of EGFR in each sample was calculated and normalized to actin. The mean values (± s.e.m.) are given.

Figure 2. AnxA6 promotes T654-EGFR phosphorylation in EGFR overexpressing cells. (**A**) A431wt and A431-A6 cells were incubated ± 10 ng/ml EGF for 3 min, subjected to EGFR immunoprecipitation and analyzed for total EGFR, pT654-EGFR, AnxA6 and PKCα as indicated. The relative amounts of PKCα and AnxA6 ± EGF in the immunoprecipitates from two independent experiments were quantified and normalized to total EGFR. The mean values (± s.e.m.) are given. (**B**) A431wt and A431-A6 cells were transfected with untagged constitutively active PKCα (CA-PKCα). Twenty-four hours after transfection, cells were starved overnight and incubated ± 10 ng/ml EGF for 3 min and subjected to EGFR immunoprecipitation as described above. Immunoprecipitates (IPs) and whole cell lysates (WCLs) were analyzed for total EGFR, pT654-EGFR, AnxA6, CA- and total PKCα as indicated. (**C**, **D**) COS-1 were grown on coverslips and co-transfected with AnxA6-CFP (**C**) or PKCα-CFP (**D**) (panels a and d) (green) and EGFR-YFP (panels b and e) (red). Twenty-four hours after transfection, cells were starved overnight and treated ± 100 ng/ml EGF for 3 min as indicated. Cells were fixed and analyzed by confocal microscopy. The merged images are shown (panels c and f). Squares with regions of interest are shown as enlarged sections with arrows indicating colocalization of AnxA6 and PKCα with EGFR in EGF stimulated cells, respectively. Bar is 10 μm. (**E**) A431wt and A431-A6 cells with stable PKCα knockdown were incubated ± 10 ng/ml EGF for 3 min. Cells stably expressing scrambled RNAi served as control (lanes 1, 3 and 4). Cell lysates were subjected to EGFR immunoprecipitation and analyzed for tyrosine phosphorylated (pY-EGFR), pT654- and total EGFR. The amount of PKCα and actin in the WCL is shown. Relative pY- and T654-EGFR phosphorylation of cells expressing scrambled RNAi (white bars) and RNAi targeting PKCα (black bars) from three independent experiments was quantified and normalized to total EGFR. The mean values (± s.e.m.) are given (*$P < 0.05$ for Student's *t*-test).

and transient actin-based protrusions on the cell surface that form in response to EGFR activation.[50] COS-1 cells co-transfected with PKCα-CFP and EGFR-YFP verified that PKCα is predominantly cytosolic in unstimulated cells and colocalizes with EGFR after EGF stimulation (Figure 2D).

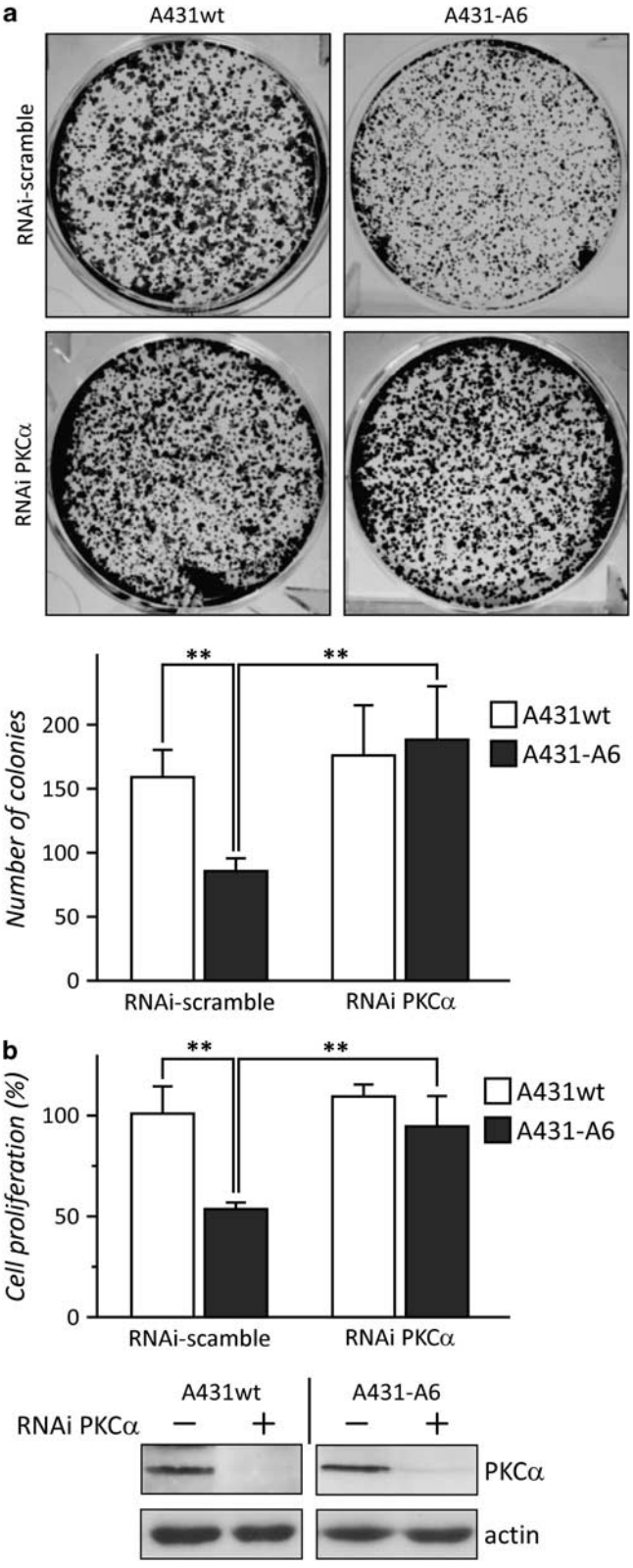

Next, we aimed to determine EGFR tyrosine and T654 phosphorylation in A431-A6 cells upon PKC depletion. Therefore, A431-A6 cells were initially incubated overnight with phorbol esters, a common pharmacological approach to attenuate PKC isozyme expression.[29] This rendered PKCα expression almost undetectable, but restored basal and EGF-inducible EGFR tyrosine phosphorylation and strongly increased Erk1/2 activation (not shown). As prolonged TPA treatment also reduces expression of other PKC isoforms,[29,51] we analyzed pY-EGFR levels in A431wt and A431-A6 cell lines after stable PKCα knockdown using RNAi (Figure 2E). Loss of PKCα did not significantly alter pY-EGFR and pT654-EGFR levels in EGF-stimulated A431wt cells compared with RNAi control (lanes 1 and 2). In contrast, PKCα depletion in A431-A6 cells reduced T654-EGFR phosphorylation, which was associated with increased EGF-inducible EGFR tyrosine phosphorylation (compare lanes 3–4 with 5–6). Similar results were obtained with catalytically inactive and dominant-negative PKCα and the PKCα inhibitor Gö6976 (data not shown).

PKCα depletion restores EGFR degradation in AnxA6 expressing A431 cells

Increased T654-EGFR phosphorylation leads to reduced EGFR internalization and degradation.[13,14] Based on the findings described above, we hypothesized decreased EGFR internalization and degradation in A431-A6 cells. To measure EGFR internalization, A431wt and A431-A6 were incubated with ^{125}I-EGF (5 ng/ml) for 5 min at 37 °C and cell surface-bound and internalized ^{125}I-EGF was determined as described.[52] Consistent with reduced EGFR activation, ^{125}I-EGF internalization was decreased in A431-A6 cells by 42 ± 4% compared with A431wt (Figure 3a). Then, EGFR protein levels were monitored in A431wt and A431-A6 cells upon stimulation with 10 ng/ml EGF for 5–30 min (Figure 3b). In EGF-treated A431wt cells, rapid EGFR degradation (33 ± 3%) was evident after 15 min (control, top panel, lanes 1–3). In contrast, EGFR protein levels remained constant in A431-A6 over this time period (control, top panel, lanes 6–10), indicating slower EGFR degradation kinetics. In PKC-depleted A431wt cells (TPA ON), 24 ± 6% EGFR degradation was detectable after 20 min (bottom panel, lanes 4 and 5). In line with the recovery of EGFR tyrosine phosphorylation after PKCα depletion (Figure 2E), 44–55% EGFR degradation occurred after 20–30 min EGF treatment in PKC-depleted A431-A6 cells (Figure 3b, TPA ON, bottom panel, lanes 9 and 10). Importantly, stable PKCα depletion effectively restored EGFR degradation kinetics in A431-A6 cells (Figure 3c, lanes 4–6), further pointing at AnxA6 levels not only determining EGFR activity, but also the intracellular fate of EGFR, in a PKCα-dependent manner.

Figure 4. PKCα depletion restores cell growth and proliferation in AnxA6 overexpressing A431 cells. (**a**) For colony forming assays, A431wt and A431-A6 cells ± stable PKCα knockdown were plated in 6-well plates (5×10^3 cells/well) and grown in DMEM, 0.1% FCS and 10 ng/ml EGF, observed twice weekly, fixed and stained as described in Materials and methods. A representative image from four independent experiments with triplicate samples is shown. Colonies containing more than ~40 cells were quantified using ImageJ software. The number of colonies (± s.d.) is given (**$P < 0.01$ for Student's *t*-test). (**b**) A431wt and A431-A6 cells ± stable PKCα knockdown were grown in 10% FCS for 72 h. Cell proliferation was monitored using an MTT assay. Mean values ± s.e.m. of five independent experiments with triplicate samples are given (**$P < 0.01$ for Student's *t*-test, respectively).

PKCα knockdown restores cell growth in A431 cells expressing AnxA6

Given that PKCα depletion restored EGFR activation in A431-A6 cells (Figure 2E), we then compared clonogenic growth of A431wt and A431-A6 cell lines with stable PKCα knockdown (Figure 4a). Cell lines stably expressing scrambled RNAi served as controls. As shown previously,[35] clonogenic growth of A431-A6 was reduced $47 \pm 6\%$ compared with controls ($^{**}P < 0.001$). Stable PKCα knockdown slightly increased the number of colonies in A431wt cells, but most noticeably, significantly increased cell growth in A431-A6 cells (2.2 ± 0.5-fold; $^{**}P < 0.001$). Likewise, colorimetric (MTT) proliferation assays confirmed $46 \pm 3\%$ decreased cell growth in A431-A6 cells (Figure 4b; $^{**}P < 0.01$), which was significantly elevated upon stable PKCα knockdown ($^{**}P < 0.01$). These findings indicate that the inhibitory effect of AnxA6 on cell growth in A431-A6 cells involves PKCα-mediated EGFR inactivation.

T654 EGFR phosphorylation is coupled to EGFR TK activity

To get mechanistic insights into AnxA6/PKCα-mediated EGFR inactivation, we investigated if T654-EGFR phosphorylation in A431-A6 cells could occur before and independent of EGFR tyrosine phosphorylation. Therefore, we next compared pY- and pT654-EGFR levels of EGFR immunoprecipitates from A431wt and A431-A6 cells preincubated with the EGFR TK inhibitor AG1478 (Figure 5a). Consistent with the data shown above (Figures 1 and 2), A431-A6 cells are characterized by reduced pY-EGFR and increased pT654-EGFR levels (compare lanes 1–4). Most strikingly, preincubation with AG1478 not only blocked EGFR tyrosine-, but also T654 phosphorylation in both cell lines. Overnight exposures confirmed increased basal T654-EGFR phosphorylation in A431-A6 cells and revealed only residual pT654-EGFR phosphorylation in both A431wt and A431-A6 cells upon preincubation with AG1478 (not shown). Hence, these findings suggest that EGFR tyrosine phosphorylation is required to enhance subsequent T654-EGFR phosphorylation in A431-A6 cells.

To further address if AnxA6/PKCα-mediated T654-EGFR phosphorylation involves EGFR tyrosine phosphorylation, we analyzed immunoprecipitates using the phosphotyrosine and pT654-EGFR-specific antibodies (Figure 5b). In line with reduced EGFR activation in A431-A6 cells, ~2-fold less pY-EGFR was immunoprecipitated from A431-A6 cells as compared with A431wt cells (compare lanes 2 and 4). pY immunoprecipitates in both cell lines also show pT654-EGFR phosphorylation, indicating that activated EGF receptors become phosphorylated at the T654 residue. Similar to the findings described above (Figures 2A and B), increased amounts of pT654-EGFR were immunoprecipitated from unstimulated and EGF-treated A431-A6 cells (Figure 5b, compare lanes 6–7 with 8–9). This pool of pT654-EGFR contained only residual amounts of phosphorylated tyrosines in both cell lines. These experiments do not fully establish a coupling of tyrosine and T654-EGFR phosphorylation in AnxA6 expressing cells and cannot discriminate if EGFR tyrosine phosphorylation is suppressed on the same EGF receptors that encounter T654 phosphorylation. Alternatively, tyrosine phosphorylation on some EGF receptors could still be responsible for increased recruitment of AnxA6/PKCα complexes to enhance subsequent T654 phosphorylation of all EGF receptors. However, these findings could indicate that EGFR tyrosine phosphorylation is followed by T654-EGFR phosphorylation. Subsequent dephosphorylation of tyrosine residues then leads to the accumulation of pT654-EGFR during EGFR inactivation.

To address if AnxA6-mediated EGFR inhibition could involve alternative pathways independent of the EGFR T654 residue, we compared the ability of AnxA6 to inhibit tyrosine phosphorylation of EGFR wild-type (WT-EGFR) and the EGFR T654A mutant (T654A-EGFR), which shows increased EGFR TK activity and cannot be inhibited by PKC.[14] To avoid interference with the high levels of endogenous EGFR in A431 cells, the comparison of WT and mutated EGFR ± AnxA6 was performed in CHO cells, which express very low/undetectable EGFR.[13,14] CHOwt with low endogenous AnxA6, and the well-characterized AnxA6 expressing CHO-A6 cell line,[29,49,53,54] were transfected with WT-EGFR and T654A-EGFR, and treated ± 100 ng/ml EGF for 3 min. Lysates were subjected to EGFR immunoprecipitation and analyzed for pY- and pT654-EGFR (Figure 5c). Similar to previous data, EGF induces tyrosine phosphorylation of WT-EGFR in CHOwt, which is associated with weak pT654-EGFR levels (lanes 1 and 2). Consistent with an increased TK activity, tyrosine phosphorylation of T654A-EGFR is already detectable in unstimulated CHOwt cells and further elevated with EGF (lanes 3 and 4). In agreement with the results described above, CHO-A6 cells exhibit very low pY- and enhanced pT654 levels of WT-EGFR (Figure 5c, lanes 5 and 6). Most strikingly, tyrosine phosphorylation of the T654A-EGFR mutant in CHO-A6 cells (lanes 7 and 8) was comparable to CHOwt, with T654A-EGFR tyrosine phosphorylation being detectable in unstimulated CHO-A6 cells and further increasing with EGF (lanes 7 and 8). Although these data do not completely rule out alternative pathways of AnxA6-mediated EGFR inactivation, such as increased recruitment of tyrosine phosphatases, it is indicative of AnxA6 inhibiting EGFR via enhanced T654-EGFR phosphorylation, possibly in a PKCα-dependent manner.

Membrane-anchored AnxA6 is a docking site for PKCα

Elevated AnxA6 levels promote PKCα membrane association (Figure 1C; Supplementary Figure S1b) and EGFR/PKCα interaction (Figures 2A and B). Previous reports showed AnxA6/PKCα interaction[28,29] and together with PKC scaffolds (RACKs, AKAP75/150, caveolin-1) recruiting PKC isoforms to membranes,[16,20,21] we hypothesized that membrane-bound AnxA6 could serve as a docking site for PKCα, possibly even in unstimulated cells. To address this question, and to avoid high endogenous EGFR levels in A431 interfering with PKCα localization studies, we first analyzed PKCα membrane association biochemically in HEK293 cells, which express only residual amounts of EGFR.[55] Therefore, membranes from control and HEK293 stably expressing AnxA6 fused to YFP and the membrane targeting sequence of K-Ras (AnxA6-YFP-tK)[56] were analyzed for PKCα membrane association. In HEK293 control cells stably expressing mCherry-tK, EGF-inducible membrane recruitment of endogenous AnxA6, PKCα and p120GAP was evident (Figure 6A, lanes 1 and 2). In contrast, elevated amounts of both membrane-bound PKCα and p120GAP in unstimulated HEK293 cells expressing membrane-tagged Anx6-YFP-tK (lane 3) were observed. Similar results were obtained from HEK293 stably expressing AnxA6 fused to the lipid anchor of H-Ras (Monastyrskaya *et al*.;[56] data not shown). Increased membrane targeting of PKCα in HEK293 cells expressing membrane-anchored AnxA6 (Anx6-YFP-tK) correlated with reduced tyrosine phosphorylation of EGFR, (pY-EGFR) and MAPK (P-Erk1/2) activation and a detectable increase in T654-EGFR phosphorylation in the presence of EGF (Figure 6B), altogether suggesting constitutive interaction of membrane-anchored AnxA6 and PKCα.

To confirm increased PKCα membrane association in cells expressing membrane-anchored AnxA6 in living cells, even in the absence of Ca^{2+}, we first analyzed mCherry-PKCα localization ± GFP-AnxA6-tK by fluorescence microscopy in HEK293 cells. However, similar to the biochemical analysis (Figure 6A, lane 1), mCherry-PKCα membrane association was already observed in unstimulated HEK293 cells not expressing membrane-anchored AnxA6. We therefore utilized an AnxA6-depleted HeLa cell line (HeLa-A6KD) described recently,[57] which express only $\sim 1.5 \times 10^5$ EGF receptors/cell[5] for further imaging studies. Cells were transfected with mCherry-PKCα and GFP-tK or GFP-AnxA6-tK, respectively (Figure 6C), starved overnight, incubated ± the

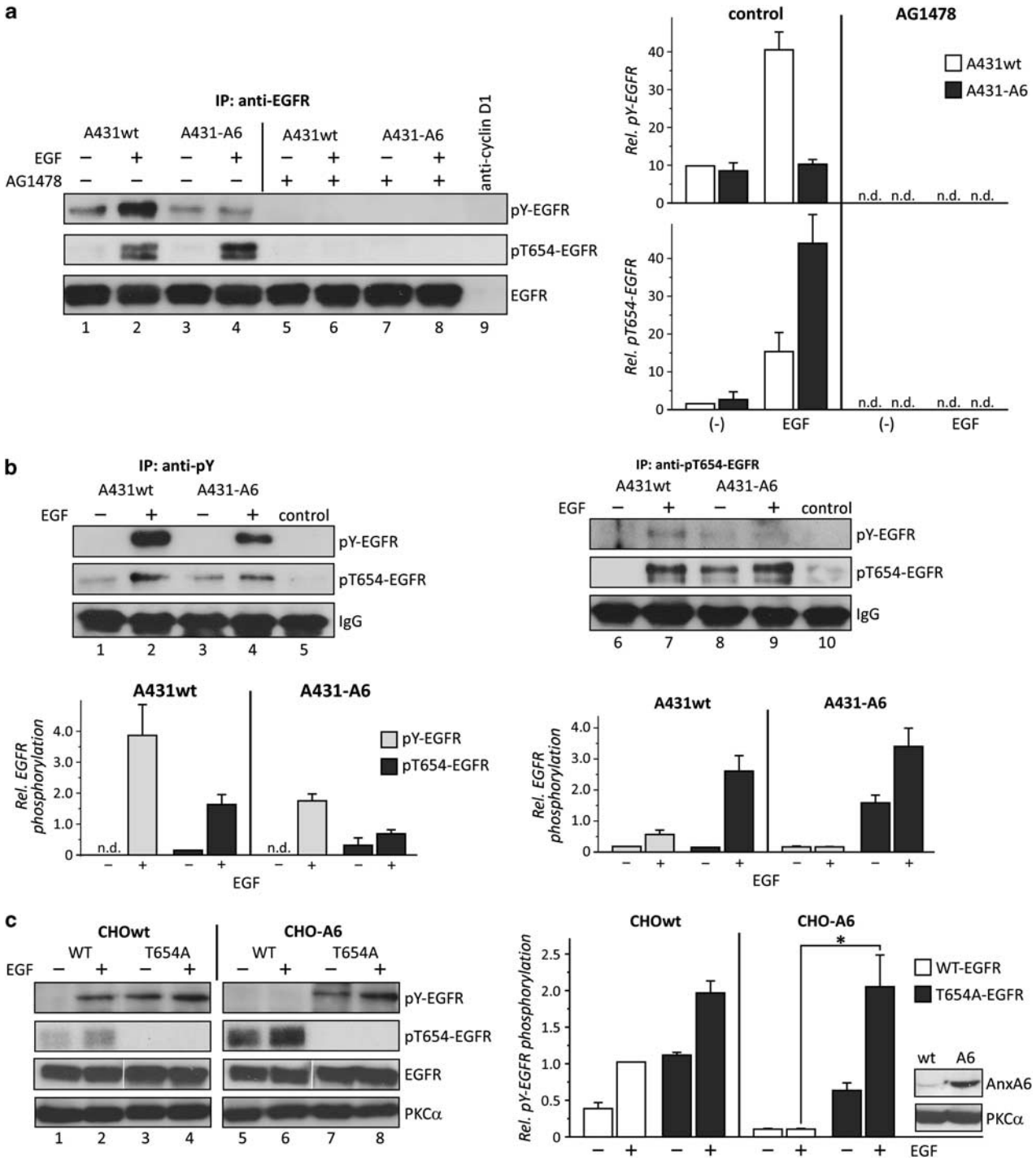

Figure 5. AnxA6 promotes T654-dependent EGFR inactivation. (**a**) Cell lysates from A431wt (lanes 1–2 and 5–6) and A431-A6 cells (lanes 3–4 and 7–8) preincubated ± AG1478 (10 μM for 60 min), followed by addition of EGF (10 ng/ml for 3 min), were immunoprecipitated with anti-EGFR and analyzed for tyrosine phosphorylation (pY-EGFR), pT654-EGFR and total EGFR by western blotting. Relative pY-EGFR and pT654-EGFR levels in A431wt and A431-A6 from two independent experiments were quantified and normalized to total EGFR. The mean values (± s.e.m.) are shown. (**b**) Cell lysates from A431wt (lanes 1 and 2) and A431-A6 cells (lanes 3 and 4) incubated ± EGF (10 ng/ml for 3 min) were immunoprecipitated with anti-pY (lanes 1–5) or anti-pT654-EGFR (lanes 6–10) and analyzed for pY-, pT654- by western blotting. Relative pY-EGFR and pT654-EGFR levels in A431wt and A431-A6 from two independent experiments were quantified. The mean values (± s.e.m.) are shown. (**c**) CHOwt and CHO-A6 cells were transfected with YFP-tagged WT EGFR and the T654A EGFR mutant (T654A). Twenty-four hours after transfection, cells were starved overnight and incubated ± 100 ng/ml EGF for 3 min as indicated. Cell lysates were subjected to EGFR immunoprecipitation and analyzed for tyrosine (pY-EGFR) and T654-EGFR phosphorylation (pT654-EGFR). The amount of total EGFR in the immunoprecipitate and PKCα and AnxA6 in the cell lysate is shown. Two different blots for PKCα and EGFR, respectively, were joined together in this presentation. The relative pY-EGFR phosphorylation of WT-EGFR (white bars) and T654A-EGFR from three independent experiments was quantified and normalized to total EGFR. The mean values (± s.e.m.) are given (*$P < 0.05$ for Student's *t*-test).

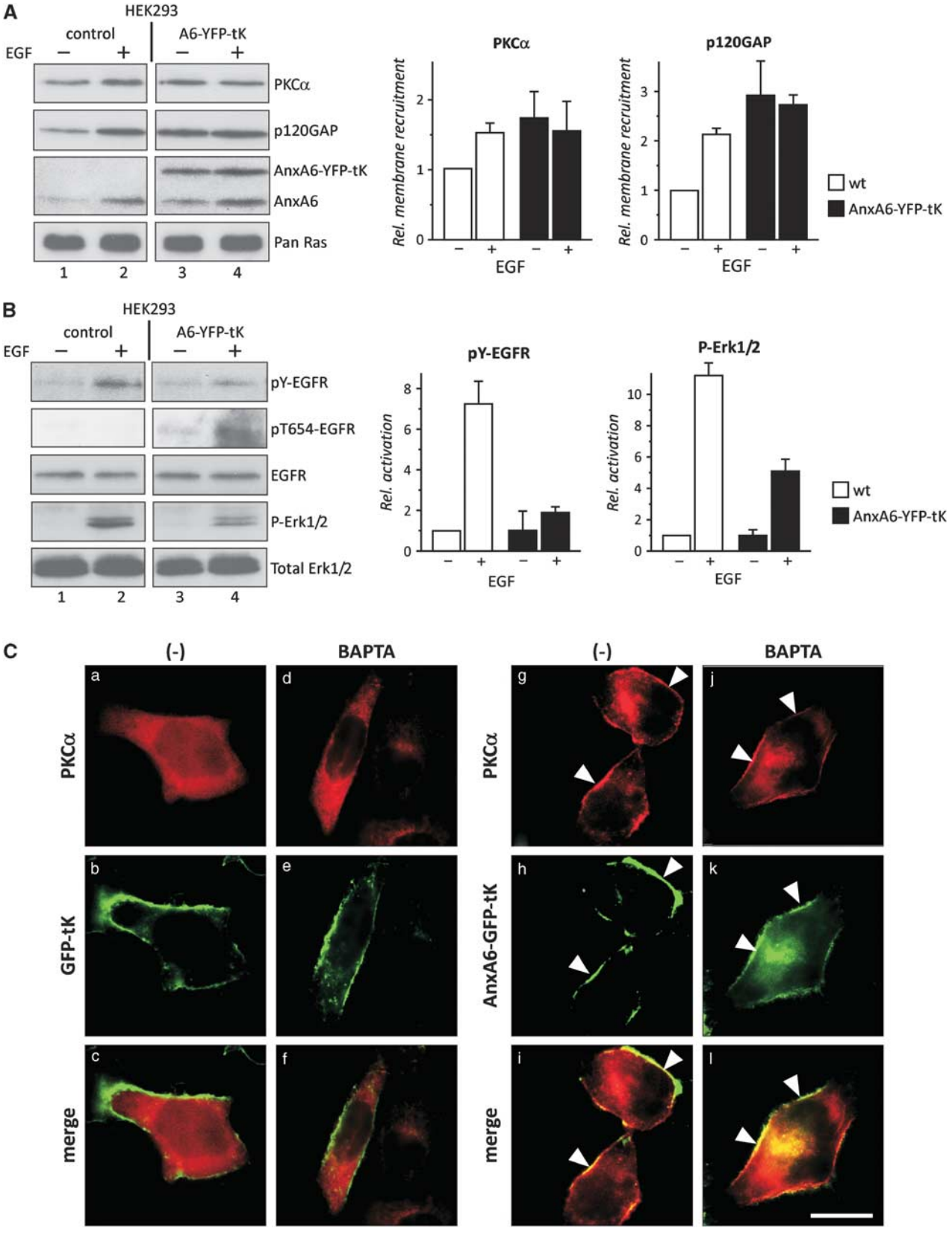

Figure 6. AnxA6 interacts and serves as a PKCα membrane docking site. (**A**, **B**) HEK293 stably expressing mCherry-tK (control, lanes 1 and 2) and AnxA6-YFP-tK cells (A6-YFP-tK, lanes 3 and 4) were incubated ± EGF (100 ng/ml) for 5 min. Crude membranes were isolated and analyzed by western blotting for (**A**) PKCα, p120GAP, AnxA6-YFP-tK, AnxA6, Pan-Ras and (**B**) activated EGFR and Erk1/2 (pY-EGFR, P-Erk1/2), pT654-EGFR, total EGFR and total Erk1/2 as indicated. (**C**) HeLa-A6KD cells were grown on coverslips and co-transfected with mCherry-PKCα (red) and GFP-tK (a–f) or AnxA6-GFP-tK (g–l, green). Twenty-four hours after transfection, cells were starved overnight, incubated ± 10 μM BAPTA-AM for 30 min, fixed and analyzed by fluorescence microscopy. The merged images are shown (panels c, f, i and l). Arrows indicate membrane localization of mCherry-PKCα in AnxA6-GFP-tK expressing cells. Bar is 10 μm.

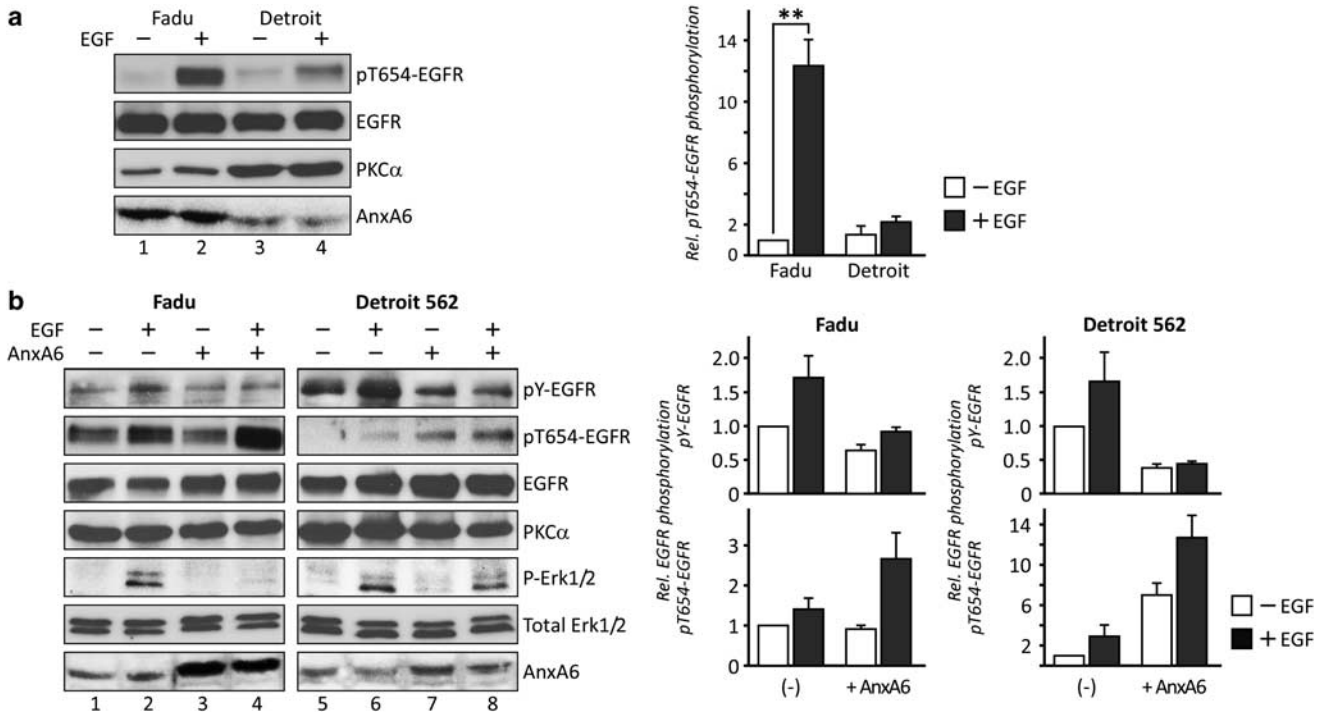

Figure 7. AnxA6 inhibits EGFR activation in EGFR overexpressing head and neck cancer cells. (**a**) Fadu and Detroit 562 were starved overnight, and incubated with 10 ng/ml EGF for 3 min as indicated. Cell lysates were analyzed for the amount of total and T654-phosphorylated EGFR (pT654-EGFR), PKCα and AnxA6. The amount of pT654-EGFR phosphorylation from three independent experiments was quantified and normalized to total EGFR. The mean values (± s.e.m.) are shown (**$P < 0.01$ for Student's *t*-test). (**b**) Fadu and Detroit 562 were transfected with AnxA6, starved overnight and incubated ± 10 ng/ml EGF for 3 min as indicated. Cell lysates were analyzed for T654-EGFR phosphorylation (pT654-EGFR), total EGFR, PKCα, activated and total Erk1/2 and AnxA6. Crude membranes from duplicate samples were analyzed for EGFR tyrosine phosphorylation (pY-EGFR). The amount of pY- and pT654-EGFR phosphorylation from two independent experiments was quantified and normalized to total EGFR. The mean values (± s.e.m.) are given.

Ca^{2+}-chelator BAPTA-AM, fixed and analyzed by fluorescence microscopy. Regardless of treatment, mCherry-PKCα was predominantly localized in the cytosol of GFP-tK expressing cells (panels a–f). In contrast, substantial amounts of mCherry-PKCα were localized at the plasma membrane in cells expressing membrane-anchored AnxA6, even after incubation with BAPTA-AM (see arrows in panels g–l).

The above findings suggested that the scaffolding function of membrane-anchored AnxA6 for PKCα might involve direct and Ca^{2+}-independent interaction. To address if constitutive interaction of endogenous AnxA6 and PKCα can occur, HeLa-A6KD and HeLa WT cells, which contain substantial amounts of AnxA6 and PKCα and show reduced T654-EGFR phosphorylation upon PKCα depletion (Supplementary Figure S2a), were compared. Similar amounts of AnxA6 were found in PKCα immunocomplexes from control and EGF-stimulated HeLa WT cells (Supplementary Figure S2b, lanes 1 and 2). Vice versa, PKCα was present in AnxA6 immunoprecipitates from control and EGF-stimulated HeLa WT cells (lanes 1 and 2), indicating that AnxA6 and PKCα can interact constitutively. In support of this interaction contributing to EGFR inactivation, we observed increased pY-EGFR and loss of both EGF-inducible pT654 EGFR phosphorylation and PKCα co-immunoprecipitation with EGFR in HeLa-A6KD cells (Supplementary Figure 2c).

AnxA6 levels modulate EGFR activation in EGFR overexpressing head and neck cancer cells

AnxA6 promotes PKCα-mediated EGFR inactivation in A431-A6 cells (Figures 1–5). To identify if AnxA6 levels modulates pT654- and pY-EGFR levels in other cell models with de-regulated EGFR, we compared EGFR overexpressing head and neck cancer cell lines (HNSCCs) Fadu and Detroit 562 (Figure 7a). Indeed, these cell lines displayed a pattern of T654-EGFR phosphorylation that was not linked to PKCα amounts, but to high and low levels of endogenous AnxA6, respectively (compare lanes 1–2 and 3–4).

We next transiently transfected Fadu and Detroit 562 with AnxA6 and determined pY- and pT654 EGFR levels ± EGF (Figure 7b). In both HNSCC lines, overexpression of AnxA6 decreased EGF-induced EGFR tyrosine phosphorylation, while pT654-EGFR levels were increased (Figure 7b, compare lanes 2, 4, 6 and 8). As shown for A431, Erk1/2 activation was strongly reduced in both Fadu and Detriot 562 ectopically expressing AnxA6 (Figure 7b). Supporting an involvement of PKCα in EGFR signaling in HNSCC, PKCα depletion (~70–80%) in Fadu cells correlated with ~50% reduced T654-EGFR phosphorylation without affecting expression of other PKC isoforms (Supplementary Figure S2a). Similarly, stable AnxA6 overexpression in EGFR overexpressing BCCs (MDA-MB-468, BT20; 35) reduced pY-EGFR, elevated pT654-EGFR levels and increased PKCα membrane association (Supplementary Figures S3a–c). Hence, AnxA6 levels modulate EGFR activity and PKCα localization in various EGFR-related cancer cell models. Interestingly, the various EGFR overexpression models (A431, HNSCC, BCCs; compare Figures 2A and 7a, Supplementary Figure S3b) and other model systems (HeLa, HEK293; see Figure 6B and Supplementary Figure S2) display fundamental differences in respect to the magnitude of basal and ligand-induced T654-EGFR phosphorylation with and without AnxA6. Taken together, this suggests that besides AnxA6 promoting PKCα/EGFR complex formation, multiple coexisting models of PKCα-mediated EGFR attenuation may exist which probably contribute differently to EGFR inactivation in the different cell lines.[16,45]

Little is known if T654-EGFR phosphorylation occurs in cancers. To get an initial insight if T654-EGFR phosphorylation possibly correlates with PKCα levels or other factors, we prepared lysates from grade 3 carcinomas ($n = 8$ per group) from luminal (ER+, progesterone receptor (PR)+, Her2−), Her2-positive (ER−, PR−) and basal (triple negative; ER−, PR−, Her2−) breast cancers. Western blotting revealed very low EGFR levels in six out of eight luminal cancers, and we therefore focused on Her2-positive and basal breast cancers, as EGFR amplification and de-regulation occurs and T654-EGFR phosphorylation was more likely to be detectable. Tissue samples were analyzed by western blotting for pT654-EGFR, total EGFR, PKCα, AnxA6, caveolin-1 and β-actin (Supplementary Figure S4). High EGFR expression levels were observed and varied 5- to 8-fold in Her2-positive and basal carcinoma, respectively. Remarkably, T654-EGFR phosphorylation was detectable in most of these human cancer biopsies. In several Her2-positive (tissue sample #2, #3 and #10) and basal carcinomas (#8, #13 and #16), significant amounts of pT654-EGFR were associated with high EGFR levels. Supporting previous data that PKCα levels do not correlate with EGFR activity/phosphorylation,[43,44] an elevated ratio of pT654-EGFR/EGFR was not associated with high PKCα levels (for example, #4, #13 and #16). Differential expression of AnxA6 and caveolin-1, which also promotes PKCα-mediated T654-EGFR phosphorylation,[16] was observed, with several samples exhibiting high pT654EGFR/EGFR ratios showing either high AnxA6 or caveolin-1 levels (#4, #5, #13 and #16). Although we were unable to observe a direct correlation between AnxA6 and pT654-EGFR levels, the heterogeneous and complex molecular entities of breast cancer subtypes might only identify correlations of AnxA6 levels with pT654-EGFR levels within small groups of certain subtypes and would require correlation studies using larger cohorts.

DISCUSSION

Here, we demonstrate that AnxA6 is a scaffold for PKCα establishing a negative feedback mechanism to downregulate ligand-induced EGFR signaling. Elevated AnxA6 levels enhance the ability of PKCα to phosphorylate T654-EGFR, which is associated with reduced EGFR tyrosine phosphorylation, internalization and degradation. AnxA6 promotes PKCα membrane targeting and PKCα/EGFR complex formation, possibly via direct interaction with both PKCα and EGFR. On the other hand, PKCα knockdown restores EGFR activation and clonogenic growth in AnxA6 expressing cells. Similarly, AnxA6 depletion increases pY-EGFR levels and reduces PKCα/EGFR interaction. Hence, the tumor suppressor activity of AnxA6 may include its ability to promote ligand-induced EGFR downregulation through increased membrane targeting of PKCα followed by EGFR/PKCα complex formation and EGFR T654 phosphorylation.

In A431, which lack endogenous AnxA6,[34,47] and other cell types, TPA-induced and PKC-mediated phosphorylation of T654-EGFR facilitates heterologous desensitization of EGF-induced EGFR signaling.[7,14] Weak T654-EGFR phosphorylation in EGF-stimulated A431 cells[41,42] made PKC an unlikely candidate to downregulate ligand-induced EGFR. Similar results were obtained in all cell lines with low AnxA6 levels in our study, including A431. Otherwise, PKC-related PNK kinases have recently been identified to facilitate constitutive T654-EGFR phosphorylation in A431wt cells, though these kinases appear to have little influence on pT654-EGFR levels in response to EGF.[45] However, Wang *et al*.[16] identified that caveolin-1 (cav-1), tetraspanin CD82 and ganglioside GM3 enabled association of EGFR with PKCα in EGF-stimulated SCC12 squamous carcinoma cells, to inhibit EGFR signaling. Some of these interactions seem cell specific and probably require GM3, CD82 and cav-1 to act as membrane organizers and stabilize the interaction of EGFR and PKCα in cholesterol-rich microdomains.[16] Alternatively, our findings suggest that AnxA6 levels determine the role of PKCα for ligand-induced EGFR downregulation in EGFR overexpressing A431, HNSCCs and BCCs, but also HeLa and HEK293 with low to moderate EGFR levels. Mechanistically, this could involve cytosolic and membrane-bound pools of AnxA6 constitutively binding to PKCα. Ca^{2+} elevation upon EGFR activation would further increase the recruitment of AnxA6 and PKCα into close proximity of EGFR. The ability of AnxA6 to interact with both PKCα and EGFR may increase the affinity of PKCα for EGFR, and establish a microenvironment promoting EGF-inducible PKCα/EGFR interaction, followed by T654-EGFR phosphorylation.

Interestingly, we recently discovered that high AnxA6 levels inhibit the exit of caveolin from the Golgi, decreasing the number of caveolae at the cell surface.[49,54] While EGFR inactivation via CD82/GM3/cav-1-dependent mechanisms is likely to occur in cholesterol-rich membrane domains,[16] AnxA6 translocates to both cholesterol-rich and -poor membrane domains.[39] Fusion of AnxA6 to membrane anchors of K- and H-Ras both increased PKCα recruitment and reduced EGFR activity. K- and H-Ras anchors (tK, tH) can target heterologous proteins (for example, GFP) to cholesterol-poor and -rich microdomains,[58] yet the A6-tK and A6-tH fusion proteins were not exclusively found in these microdomains in subcellular fractionations (data not shown), indicating that the Ca^{2+}, phospholipid and cholesterol binding ability of AnxA6 contributes to membrane microlocalization. However, one can envisage that fine-tuning of AnxA6 and cav-1 expression and microlocalization might downregulate different EGFR effector pathways, as recruitment of PKCα via AnxA6 or CD82/GM3/cav-1 could target dissimilar pools of activated EGFR in different microdomains at the cell surface.

The spatio-temporal targeting of PKC isozymes to unique subcellular localizations is complex and involves diacylglycerol, Ca^{2+}, lipid binding through their C1 and C2 domains and scaffold proteins.[18,19,21] The PKC scaffolds RACK and AKAP79/150 are membrane associated and only recruit activated PKC isozymes. AKAP79/150 interacts with multiple PKC isozymes,[59,60] RACK1 and RACK2 selectively bind PKCβ and PKCε via their C2 domains, respectively.[18,21] Likewise, AnxA5 binds to the C2 domain of PKCδ,[25] but AnxA5/PKCδ assembly precedes PKCδ membrane translocation and function. Similarly, AnxA6 (i) constitutively interacts with PKCα, (ii) increases PKCα membrane association and (iii) serves as a PKCα membrane docking site even in unstimulated cells. The AnxA6 linker, which separates AnxA6 annexin repeats 1–4 from 5–8, contains a PKC phosphorylation site at T356[61] and constitutively binds to C2 domains of other proteins, such as p120GAP.[33–35] In addition, we showed that a deletion mutant lacking the AnxA6 linker region and C-terminal Anx repeats cannot promote PKCα membrane recruitment.[29] Consistent with these findings, overexpression of this mutant in A431 cells did not promote T654-EGFR phosphorylation or EGFR/PKCα complex formation. Therefore, the C2 domain of PKCα might be critical for membrane association not only through Ca^{2+} sensing and phospholipid binding, but also via a unique AnxA6/PKCα interaction. Alternatively, Kirsch and coworkers recently mapped the AnxA6/PKCα interaction within the AnxA6 C-terminus.[62] Hence, AnxA5 and AnxA6 may represent a new class of PKC scaffolds that can interact with PKC isozymes before cell activation, possibly ensuring rapid and site-specific membrane targeting of PKC isozymes from the cytosol upon activation.

We previously demonstrated that AnxA6 interacts with p120GAP and active H-Ras to promote p120GAP/H-Ras assembly and Ras/MAPK inhibition in EGFR overexpressing A431 and BCCs.[34,35,38] In addition, AnxA6 can interact with PKCα and EGFR to downregulate EGFR activation. Together with AnxA6 co-purifying with Raf-1,[36] the scaffolding function of AnxA6 may involve multiple protein–protein interactions and the recruitment of at least two regulators, p120GAP and PKCα, to EGFR and Ras. Several other EGFR/Ras/MAPK scaffolds also have multiple interaction partners. IQGAP1 binds to EGFR, B-Raf, Mek/Erk kinases

and is required for maximal MAPK activation.[32] Kinase Suppressor of Ras binds to C-Raf, Mek1/2, Erk1/2 and Kinase Suppressor of Ras levels determine the magnitude of MAPK activation.[31] High amounts of AnxA6 might enable multiple, possibly simultaneous, interactions with different members of the EGFR/Ras/MAPK pathway to ensure signal termination. Differential expression, localization and recruitment of scaffolds that either stabilize or terminate EGFR/Ras/MAPK signaling could thereby integrate diverse signaling pathways and multiple cellular activities. Expression analysis of Her2-positive and basal breast carcinoma did not reveal an association between T654-EGFR phosphorylation and PKCα levels, confirming previous studies[43,44] and further indicating that scaffolds, such as AnxA6 and caveolin-1,[16] or even other kinases,[45] may contribute to EGFR inactivation.

AnxA6 is downregulated in EGFR overexpressing and ER-negative BCCs. In these cells, elevation of AnxA6 reduced cell growth, whereas AnxA6 depletion increased transformation efficiency.[35] Decreased AnxA6 levels in human breast carcinoma,[40] and reduced growth of A431 cells ectopically expressing AnxA6 in mouse xenografts,[63] further suggest tumor suppressor activity of AnxA6 in cells with de-regulated EGFR and elevated WT (hyperactive) Ras activity. The ability of AnxA6 to promote PKCα-dependent EGFR inactivation in EGFR overexpressing A431, BCCs and HNSCC supports anti-proliferative properties of AnxA6 in certain susceptible cell types and co-operating genetic lesions, such as EGFR overexpression. Loss of 5q31-35, which contains the AnxA6 locus, is common in ER-negative breast tumors that carry *ErbB2* gene amplifications, which have strong oncogenic potential.[64,65] Deletion of 5q31-32, which contains around 40 genes, some of those, including AnxA6, with tumor suppressor properties,[66] is also associated with the myelodysplastic syndrome and acute myelogenous leukemia. It should also be noted that alternative splicing gives rise to two AnxA6 isoforms. While full-length AnxA6-1 is the predominant isoform in most tissues, increased levels of the shorter AnxA6-2 isoform lacking 524-VAAEIL-529 were found in some immortalized cell lines. It is unclear if the two isoforms fulfill different roles in tumorigenesis, but recent studies indicate different localization and regulation of AnxA6 isoforms.[67,68] Alternatively, AnxA6 promoter methylation in A431wt and MDA-MB-468[35] suggests that enhanced EGFR and Ras/MAPK signaling might downregulate AnxA6 through epigenetic silencing.

Upregulation of PKCα has long been implicated in ER-negative breast cancers.[44,68,69] Consistent with published data,[70,71] we observed very low PKCα levels in a panel of ER-positive BCCs, while the majority of ER-negative BCCs contained significant amounts of PKCα (data not shown). Interestingly, ER-positive BCCs express substantial amounts of AnxA6, but most ER-negative BCCs express low to modest amounts of AnxA6,[35] indicating that loss of AnxA6 enables PKCα to target substrates other than EGFR, possibly leading to oncogenic signaling events.

Increasing evidence suggests that scaffold proteins regulating PKC isozyme localization provide exciting opportunities for therapeutic intervention. Peptides interfering with the interaction of PKC isoforms and their respective scaffolds can inhibit PKC membrane targeting and activity in cells and animal models of human disease.[21,25] Recently, a short and PKCα-specific peptide inhibitor (Q***L***VI***A***N) with similarities to the AnxA6 linker between Pos. 341 and 346 (E***L***SAV***A***), reduced breast cancer metastasis, but not primary tumor growth in mice.[44] Similar approaches will provide opportunities to investigate if tumor suppressor activity of AnxA6 in EGFR overexpressing cells is mediated via the potential scaffolding function of the AnxA6 linker region.

MATERIALS AND METHODS

Reagents and antibodies

DMEM, DMEM/F12, RPMI-1640, Ham's F-12, trypsin, L-glutamine, penicillin, streptomycin, Percoll and 4,6-diamidino-2-phenylindole dihydrochloride were from Invitrogen (Mulgrave, Victoria, Australia). Geneticin (G418), Mowiol and human recombinant EGF were from Merck (Frenchs Forest, NSW, Australia). BAPTA-AM, Ionomycin, 2-mercaptoethanol, 12-O-tetradecanoyl-phorbol-13-acetate (TPA), paraformaldehyde, Insulin, Gö6976, AG1478 and sucrose were from Sigma (Caste Hill, NSW, Australia). ^{125}I-EGF and Protein G sepharose were from GE Healthcare (Chalfont, St Giles, UK). Mono- and polyclonal antibodies against EGFR, rabbit anti-pT654-EGFR were from Santa Cruz (Santa Cruz, CA, USA). Mouse monoclonal antibodies against PKCα, PKCβ, PKCδ, PKCε and PKCι, Pan Ras, p120GAP, and rabbit anti-caveolin were from BD Transduction Laboratories (Lexington, KY, USA). Antibodies against phosphotyrosine (mouse), activated Erk1/2 (P-Erk1/2; mouse), Total Erk1/2 (rabbit) and β-actin (rabbit) were from Cell Signalling (Beverly, MA, USA). The rabbit anti-AnxA6 antibody was prepared in our laboratory.[48,53] Expression vectors encoding EGFP-AnxA6, AnxA6-CFP, and EGFP- or YFP-AnxA6 ± the lipid anchors of H- and K-Ras (AnxA6-YFP-tK, AnxA6-YFP-tH, AnxA6-EGFP-tK) have been described.[35,53,56] The plasmid expressing inactive PKCα (DN-PKCα) contains the bovine PKCα cDNA mutated at codon 368 from AAG (L) to AGA (R).[29] The constitutively active PKCα mutant (CA-PKCα) is a pseudosubstrate site deletion in the bovine PKCα cDNA removing codons 22–28 (RLGALRQ). Mutant and WT PKCα PCR fragments were cloned into pCRblunt (Invitrogen) and sequenced. For mCherry-PKCα, the cDNA was cloned into pEGFP-C1, where EGFP was replaced with mCherry. For CFP-tagged PKCα, the human PKCα cDNA was cloned into pCFP-C1. Plasmids encoding GFP-tH, GFP-tK, EGFP-EGFR, YFP-EGFR and YFP-T654A-EGFR were kindly provided by J Hancock (Dallas, USA) and A Sorkin (Pittsburgh, USA), respectively. Cy3- and Cy5- conjugated secondary antibodies were from Molecular Probes (Eugene, OR, USA) and Jackson ImmunoResearch (Westgrove, PA, USA). Horseradish Peroxidase-labeled antibodies and SDS–PAGE molecular weight markers were from Cell Signalling. The breast cancer samples used in this study were provided by the Victorian Cancer Biobank, which is supported by the Victorian Government. The project was approved by the St Vincent's Hospital Sydney human research ethics committee (approval number HREC 08/145). All breast cancer samples were grade 3 carcinoma and classified by immunohistochemistry as luminal (ER+, PR+, Her2−), Her2-positive (ER−, PR−) and basal (triple negative: ER−, PR−, Her2−).

Cell culture

A431wt, A431-A6, HeLa, HeLa-A6KD, COS-1 and HEK293 were grown in DMEM, Fadu and Detroit 562 in DMEM/F12, CHOwt and CHO-A6 in Ham's F12, together with 10% fetal calf serum (FCS), L-glutamine (2 mM), penicillin (100 U/ml) and streptomycin (100 μg/ml) at 37 °C, 5% CO_2. MDA-MB-468, BT20 were grown in RPMI-1640 together with Insulin (0.3 U/ml) and FCS, glutamine, penicillin and streptomycin as above. For the generation of stable A431 cells expressing the AnxA6 mutant $A6_{1-175}$, A431wt cells were transfected with pcDNAAnx6_{1-175} and selected in the presence of 1 mg/ml G418 as described.[35,53] After 2 weeks G418-resistant and $A6_{1-175}$ expressing colonies were identified. The generation of A431, MDA-MB-468, BT20 and CHO cell lines stably expressing AnxA6 and HEK293 stably expressing Anx6-YFP-tK has been described.[34–36,53,56]

Suppression of PKCα and AnxA6 expression by RNAi

For stable PKCα and AnxA6 knockdown in A431 and HeLa, 1–2 × 10^6 cells were transfected with 1.5 μg SureSilencing shRNA plasmid (SABiosciences, Doncaster, Victoria, Australia) targeting human PKCα at Pos. 1606–1626 (5′-cctccatttgatggtgaagat-3′) or human AnxA6 at Pos. 352–372 (5′-gcaaggacctcattgctgatt-3′) together with Lipofectamine 2000 (Invitrogen), according to manufacturer's instructions. After 48 h, cells were selected with 1.5 μg/ml puromycin. After 2 weeks, puromycin-resistant and PKCα- or AnxA6-depleted colonies were identified. Stable A431wt, A431-A6 and HeLa cell lines expressing scrambled RNAi (5′-ggaatctcattcgatgcatac-3′) served as negative controls. For transient PKCα depletion, 1–2 × 10^5 cells were transfected in 2 ml media with 1.5 μg PKCα or scrambled shRNA plasmid and Lipofectamine 2000 as above. Lysates were prepared 72 h after transfection and analyzed for PKCα depletion (~70–90%) and EGFR phosphorylation.

Growth assays

Colony forming assays were performed as described.[72] Cells were fixed and stained with Diff Quick stain (Lab Aids, Australia). Images were captured using a Leica DMI3000B microscope (Leica Microsystems, North Ryde, NSW,

Australia). Colonies with >40 cells were quantified using ImageJ (version 1.42; NIH, Bethesda, MA, USA) particle analysis mode.

Cell proliferation was determined using a colorimetric (MTT; 3-(4,5-dimethylthiazol-2-yl)-2,5-diphenyltetrazolium bromide) assay according to manufacturer's instructions. Cells (2×10^3, in triplicate) were grown in 10% FCS for 72 h. Cells were incubated with 20 μl of MTT (5 mg/ml) for 60 min, the media was removed and spectrophotometric absorbance of samples in dimethyl sulfoxide was measured at 550 nm (Microplate Reader, Model 689, Bio-Rad, Hercules, CA, USA) with a reference filter of 655 nm. All experiments were performed in triplicate in at least three separate experiments.

Subcellular fractionation

Crude membranes from cells were prepared as described previously.[35,73] In brief, cells lysed in 10 mM Tris–HCl (pH 7.5), 5 mM $MgCl_2$, 1 mM EGTA, 1 mM DTT and protease inhibitors were homogenized and nuclei were removed by low speed centrifugation. Postnuclear supernatants were spun at 100 000 *g* at 4 °C for 30 min and membrane pellets were resuspended by sonication in 50 μl of lysis buffer. Aliquots were analyzed by western blotting for total and phosphorylated EGFR, PKCα, p120GAP, Ras and AnxA6.

Plasma membrane-enriched fractions were isolated from Percoll gradients as described.[34] In all, 1×10^7 cells were washed in 0.25 M sucrose, 1 mM EDTA, 20 mM Tris–HCl, pH 7.8 plus protease inhibitors, collected and centrifuged. The postnuclear supernatant was layered on top of 8 ml of 30% Percoll and centrifuged at 84 000 *g* for 30 min in a Beckman 70.1 TI rotor (Gladesville, NSW, Australia). In all, 1 ml fractions from top to bottom were collected (plasma membrane in fractions 3–5), concentrated and analyzed for the amount of EGFR and Ras.

Internalization of ^{125}I-EGF

The internalization of ^{125}I-radiolabeled EGF was measured as described previously.[52] In all, 1×10^6 cells were incubated with 1 ng/ml ^{125}I-EGF for 5 min at 37 °C. Non-internalized I^{125}-EGF was removed with acid wash and cells were lysed in 0.1 N NaOH to measure the amount of cell surface-bound and internalized ^{125}I-EGF, respectively. The ratio of internalized and surface-bound ^{125}I-EGF was calculated and mean values (± s.e.m.) from three independent experiments with triplicate samples are given.

Immunoprecipitation

Immunoprecipitations were performed as described.[35,74] In all, 1×10^7 cells were starved overnight, washed twice in phosphate-buffered saline and scraped in 0.5 ml of lysis buffer (20 mM HEPES pH 7.2, 1% NP-40, 10% Glycerol (v/v), 50 mM NaF, 1 mM PMSF, 1 mM Na_3VO_4, 10 μg/ml leupeptin and 2 μg/ml aprotinin). The protein content was determined and 800–1000 μg of cell lysate was incubated with 2 μg of anti-EGFR (mouse), anti-phosphotyrosine (mouse), anti-pT654-EGFR (rabbit), anti-PKCα (mouse), anti-AnxA6 (rabbit), or control mouse/rabbit antibody overnight at 4 °C. Samples were added to Protein G sepharose and incubated for 2 h at 4 °C, centrifuged and washed four times in lysis buffer. The immunoprecipitates were analyzed for EGFR, pY-EGFR, pT654-EGFR, PKCα and AnxA6.

Immunofluorescence

Cells were seeded at 1×10^5/ml and grown on coverslips. In some experiments, cells were transfected with plasmids encoding AnxA6, PKCα or EGFR with Lipofectamine as described above. Twenty-four hours after transfection, cells were starved overnight and incubated with 10 μM BAPTA-AM for 30 min, or activated with EGF (10–100 ng/ml) or ionomycin (2 μM) for 3 min, washed with cold phosphate-buffered saline and fixed with 4% paraformaldehyde (or methanol for anti-pT654-EGFR). Cells were washed, permeabilized with 0.1% saponin and incubated with first and secondary antibodies as described.[49,54] EGFR, pT654-EGFR and phosphotyrosine were visualized using mouse anti-EGFR, rabbit anti-pT654-EGFR and mouse anti-phosphotyrosine as first and Cy3- and Cy5-donkey anti-mouse or rabbit (Cy3) as secondary antibodies (Jackson ImmunoResearch). Samples were washed extensively and coverslips were mounted with Mowiol (Merck). Localization of EGFR, PKCα and AnxA6 was studied using a Leica DMI3000B inverted fluorescent microscope and images were collected with IPLab Gel software (Leica Microsystems). In some experiments, images were analyzed with a Leica TCS SP5 laser scanning confocal microscope (Leica Microsystems, Heidelberg, Germany) equipped with an APO ×63 oil immersion objective lens. Image analysis and manipulation was performed with ImageJ NIH image software (NIH).

Western blot analysis

Cell and tissue lysates and samples from immunoprecipitations and membrane preparations were separated by 8–12.5% SDS–PAGE and transferred onto Immobilon-P (Millipore, Billerica, MA, USA). Proteins were detected using their specific primary antibodies, followed by horseradish peroxidase-conjugated secondary antibodies and enhanced chemiluminescence detection (ECL, Perkin-Elmer, Glen Waverly, Victoria, Australia).

CONFLICT OF INTEREST

The authors declare no conflict of interest.

ACKNOWLEDGEMENTS

This study was supported by grants to TG from the National Health and Medical Research Council of Australia (NHMRC; 510293, 510294) and the University of Sydney (2010-02681). CE is supported by BFU2009-10335, Consolider-Ingenio CSD2009-00016 from Ministerio de Innovación, Ciencia y Tecnología and PI040236 from Fundació Marató TV3 (Barcelona, Spain). FT is supported by BFU2009-13526. RJD and AS would like to acknowledge funding from the NHMRC. PW is a recipient of a co-funded National Heart Foundation (NHF)/NHMRC postgraduate scholarship. CR is grateful to the Beatriu de Pinós fellowship (Generalitat de Catalunya). SV is thankful to Ministerio de Educación y Ciencia, Spain, (FPI mobility Program) for a short-term fellowship at the laboratory of TG (Sydney, Australia). MR and AA are supported by fellowships from Ministerio de Innovación, Ciencia y Tecnología. AS is supported by Early Career Fellowships from the Cancer Institute NSW and the National Breast Cancer Foundation.

REFERENCES

1 Pines G, Koestler WJ, Yarden Y. Oncogenic mutant forms of EGFR: lessons in signal transduction and targets for cancer therapy. *FEBS Lett* 2010; **584**: 2699–2706.
2 Warren CM, Landgraf R. Signalling through ERBB receptors: multiple layers of diversity and control. *Cell Signal* 2006; **18**: 923–933.
3 Ferguson KM. Structure-based view of epidermal growth factor receptor regulation. *Annu Rev Biophys* 2008; **37**: 353–373.
4 Lanzetti L, Di Fiore PP. Endocytosis and cancer: an 'insider' network with dangerous liaisons. *Traffic* 2008; **9**: 2011–2021.
5 Sorkin A, Goh LK. Endocytosis and intracellular trafficking of ErbBs. *Exp Cell Res* 2008; **314**: 3093–3106.
6 Hunter T, Ling N, Cooper JA. Protein kinase C phosphorylation of the EGF receptor at a threonine residue close to the cytoplasmic face of the plasma membrane. *Nature* 1984; **311**: 480–483.
7 Davis RJ, Czech MP. Platelet-derived growth factor mimics phorbol diester action on epidermal growth factor receptor phosphorylation at threonine-654. *Proc Natl Acad Sci USA* 1985; **82**: 4080–4084.
8 Livneh E, Dull TJ, Berent E, Prywes R, Ullrich A, Schlessinger J. Release of a phorbol ester-induced mitogenic block by mutation at Thr-654 of the epidermal growth factor receptor. *Mol Cell Biol* 1988; **8**: 2302–2308.
9 Friedman BA, van Amsterdam J, Fujiki H, Rosner MR. Phosphorylation at threonine-654 is not required for negative regulation of the epidermal growth factor receptor by non-phorbol tumor promoters. *Proc Natl Acad Sci USA* 1989; **86**: 812–816.
10 Countaway JL, McQuilkin P, Girones N, Davis RJ. Multisite phosphorylation of the epidermal growth factor receptor. Use of site-directed mutagenesis to examine the role of serine/threonine phosphorylation. *J Biol Chem* 1990; **265**: 3407–3416.
11 Bowen S, Stanley K, Selva E, Davis RJ. Constitutive phosphorylation of the epidermal growth factor receptor blocks mitogenic signal transduction. *J Biol Chem* 1991; **266**: 1162–1169.
12 Morrison P, Takishima K, Rosner MR. Role of threonine residues in regulation of the epidermal growth factor receptor by protein kinase C and mitogen-activated protein kinase. *J Biol Chem* 1993; **268**: 15536–15543.
13 Lund KA, Lazar CS, Chen WS, Walsh BJ, Welsh JB, Herbst JJ *et al.* Phosphorylation of the epidermal growth factor receptor at threonine 654 inhibits ligand-induced internalization and down-regulation. *J Biol Chem* 1990; **265**: 20517–20523.
14 Bao J, Alroy I, Waterman H, Schejter ED, Brodie CH, Gruenberg J *et al.* Threonine phosphorylation diverts internalized epidermal growth factor receptors from a degradative pathway to the recycling endosome. *J Biol Chem* 2000; **275**: 26178–26186.

15 Santiskulvong C, Rozengurt E. Protein kinase Calpha mediates feedback inhibition of EGF receptor transactivation induced by Gq-coupled receptor agonists. *Cell Signal* 2007; **19**: 1348–1357.
16 Wang XQ, Yan Q, Sun P, Liu JW, Go L, McDaniel SM *et al.* Supression of epidermal growth factor receptor signaling by protein kinase C-alpha activation requires CD82, caveolin-1, and ganglioside. *Cancer Res* 2007; **67**: 9986–9995.
17 Prevostel C, Alice V, Joubert D, Parker PJ. Protein kinase Çalphą actively down-regulates through caveolae-dependent traffic to an endosomal compartment. *J Cell Sci* 2000; **113**: 2575–2584.
18 Steinberg SF. Structural basis of protein kinase C isoform function. *Physiol Rev* 2008; **88**: 1341–1378.
19 Groves JT, Kuriyan J. Molecular mechanisms in signal transduction at the membrane. *Nat Struct Mol Biol* 2010; **17**: 659–665.
20 Mochly-Rosen D. Localization of protein kinases by anchoring proteins: a theme in signal transduction. *Science* 1995; **268**: 247–251.
21 Kheifets V, Mochly-Rosen D. Insight into intra- and inter-molecular interactions of PKC: design of specific modulators of kinase function. *Pharm Res* 2007; **55**: 467–476.
22 Dubois T, Oudinet JP, Mira JP, Russo-Marie F. Annexins and protein kinases C. *Biochim Biophys Acta* 1996; **1313**: 290–294.
23 Gerke V, Creutz CE, Moss SE. Annexins: linking Ca2+ signalling to membrane dynamics. *Nat Rev Mol Cell Biol* 2005; **6**: 449–461.
24 Grewal T, Enrich C. Annexins - modulators of EGF receptor signalling and trafficking. *Cell Signal* 2009; **21**: 847–858.
25 Kheifets V, Bright R, Inagaki K, Schechtman D, Mochly-Rosen D. Protein kinase C delta (deltaPKC)-annexin V interaction: a required step in deltaPKC translocation and function. *J Biol Chem* 2006; **281**: 23218–23226.
26 Ron D, Mochly-Rosen D. Agonists and antagonists of protein kinase C function, derived from its binding proteins. *J Biol Chem* 1994; **269**: 21395–21398.
27 Xu TR, Rumsby MG. Phorbol ester-induced translocation of PKC epsilon to the nucleus in fibroblasts: identification of nuclear PKC epsilon-associating proteins. *FEBS Lett* 2004; **570**: 20–24.
28 Schmitz-Peiffer C, Browne CL, Walker JH, Biden TJ. Activated protein kinase C alpha associates with annexin VI from skeletal muscle. *Biochem J* 1998; **330**: 675–681.
29 Rentero C, Evans R, Wood P, Tebar F, Vilà de Muga S, Cubells L *et al.* Inhibition of H-Ras and MAPK is compensated by PKC-dependent pathways in annexin A6 expressing cells. *Cell Signal* 2006; **218**: 1006–1016.
30 Grewal T, Tebar F, Pol A, Enrich C. Involvement of targeting and scaffolding proteins in the regulation of the EGFR/Ras/MAPK pathway in oncogenesis. *Curr Signal Transduct Ther* 2006; **1**: 147–167.
31 Clapéron A, Therrien M. KSR and CNK: two scaffolds regulating RAS-mediated RAF activation. *Oncogene* 2007; **26**: 3143–3158.
32 McNulty DE, Li Z, White CD, Sacks DB, Annan RS. MAPK scaffold IQGAP1 binds the EGF receptor and modulates its activation. *J Biol Chem* 2011; **286**: 15010–15021.
33 Davis AJ, Butt JT, Walker JH, Moss SE, Gawler DJ. The Ca2+-dependent lipid binding domain of P120GAP mediates protein-protein interactions with Ca2+-dependent membrane-binding proteins. Evidence for a direct interaction between annexin VI and P120GAP. *J Biol Chem* 1996; **271**: 24333–24336.
34 Grewal T, Evans R, Rentero C, Tebar F, Cubells L, de Diego I *et al.* Annexin A6 stimulates the membrane recruitment of p120GAP to modulate Ras and Raf-1 activity. *Oncogene* 2005; **24**: 5809–5820.
35 Vilà de Muga S, Timpson P, Cubells L, Evans R, Hayes TE, Rentero C *et al.* Annexin A6 inhibits Ras signalling in breast cancer cells. *Oncogene* 2009; **28**: 363–377.
36 Pons M, Tebar F, Kirchhoff M, Peiró S, de Diego I, Grewal T *et al.* Activation of Raf-1 is defective in annexin 6 overexpressing Chinese hamster ovary cells. *FEBS Lett* 2001; **501**: 69–73.
37 Blagoev B, Kratchmarova I, Ong SE, Nielsen M, Foster LJ, Mann M. A proteomics strategy to elucidate functional protein-protein interactions applied to EGF signaling. *Nat Biotechnol* 2003; **21**: 315–318.
38 Grewal T, Koese M, Rentero C, Enrich C. Molecules in focus: Annexin A6 – regulator of the EGFR/Ras signalling pathway and cholesterol homeostasis. *Int J Biochem Cell Biol* 2010; **42**: 580–584.
39 Enrich C, Rentero C, de Muga SV, Reverter M, Mulay V, Wood P *et al.* Annexin A6 – linking Ca(2+) signaling with cholesterol transport. *Biochim Biophys Acta* 2011; **1813**: 935–947.
40 Sakwe AM, Koumangoye R, Guillory B, Ochieng J. Annexin A6 contributes to the invasiveness of breast carcinoma cells by influencing the organization and localization of functional focal adhesions. *Exp Cell Res* 2011; **317**: 823–837.
41 King CS, Cooper JA. Effects of protein kinase C activation after epidermal growth factor binding on epidermal growth factor receptor phosphorylation. *J Biol Chem* 1986; **261**: 10073–10078.
42 Iwashita S, Fox CF. Epidermal growth factor and potent phorbol tumor promoters induce epidermal growth factor receptor phosphorylation in a similar but distinctively different manner in human epidermoid carcinoma A431 cells. *J Biol Chem* 1984; **259**: 2559–2567.
43 Fabbro D, Küng W, Roos W, Regazzi R, Eppenberger U. Epidermal growth factor binding and protein kinase C activities in human breast cancer cell lines: possible quantitative relationship. *Cancer Res* 1986; **46**: 2720–2725.
44 Kim J, Thorne SH, Sun L, Huang B, Mochly-Rosen D. Sustained inhibition of PKCα reduces intravasation and lung seeding during mammary tumor metastasis in an *in vivo* mouse model. *Oncogene* 2011; **30**: 323–333.
45 Collazos A, Michael N, Whelan RD, Kelly G, Mellor H, Pang LC *et al.* Site recognition and substrate screens for PKN family proteins. *Biochem J* 2011; **438**: 535–543.
46 Rikova K, Guo A, Zeng Q, Possemato A, Yu J, Haack H *et al.* Global survey of phosphotyrosine signaling identifies oncogenic kinases in lung cancer. *Cell* 2007; **131**: 1190–1203.
47 Smythe E, Smith PD, Jacob SM, Theobald J, Moss SE. Endocytosis occurs independently of annexin VI in human A431 cells. *J Cell Biol* 1994; **124**: 301–306.
48 de Diego I, Schwartz F, Siegfried H, Dauterstedt P, Heeren J, Beisiegel U *et al.* Cholesterol modulates the membrane binding and intracellular distribution of annexin 6. *J Biol Chem* 2002; **277**: 32187–32194.
49 Cubells L, Vilà de Muga S, Tebar F, Wood P, Evans R, Ingelmo-Torres M *et al.* Annexin A6-induced alterations in cholesterol transport and caveolin export from the Golgi complex. *Traffic* 2007; **8**: 1568–1589.
50 Orth JD, Krueger EW, Weller SG, McNiven MA. A novel endocytic mechanism of epidermal growth factor receptor sequestration and internalization. *Cancer Res* 2006; **66**: 3603–3610.
51 Stewart JR, O'Brien CA. Protein kinase C-(alpha) mediates epidermal growth factor receptor transactivation in human prostate cancer cells. *Mol Cancer Ther* 2005; **4**: 726–732.
52 Tebar F, Villalonga P, Sorkina T, Agell N, Sorkin A, Enrich C. Calmodulin regulates intracellular trafficking of epidermal growth factor receptor and the MAPK signaling pathway. *Mol Biol Cell* 2002; **13**: 2057–2068.
53 Grewal T, Heeren J, Mewawala D, Schnitgerhans T, Wendt D, Salomon G *et al.* Annexin VI stimulates endocytosis and is involved in the trafficking of LDL to the prelysosomal compartment. *J Biol Chem* 2000; **275**: 33806–33813.
54 Cubells L, Vilá de Muga S, Tebar F, Bonventre JV, Balsinde J, Pol A *et al.* Annexin A6-induced inhibition of cytoplasmic phospholipase A2 is linked to caveolin export from the Golgi. *J Biol Chem* 2008; **283**: 10174–10183.
55 Stern KA, Visser Smit GD, Place TL, Winistorfer S, Piper RC, Lill NL. Epidermal growth factor receptor fate is controlled by Hrs tyrosine phosphorylation sites that regulate Hrs degradation. *Mol Cell Biol* 2007; **27**: 888–898.
56 Monastyrskaya K, Babiychuk EB, Hostettler A, Wood P, Grewal T, Draeger A. Plasma membrane-associated annexin A6 reduces Ca2+ entry by stabilizing the cortical actin cytoskeleton. *J Biol Chem* 2009; **284**: 17227–17242.
57 Reverter M, Rentero C, de Muga SV, Alvarez-Guaita A, Mulay V, Cairns R *et al.* Cholesterol transport from late endosomes to the Golgi regulates t-SNARE trafficking, assembly, and function. *Mol Biol Cell* 2011; **22**: 4108–4123.
58 Apolloni R, Prior IA, Lindsay M, Parton RG, Hancock JF. H-ras but not K-ras traffics to the plasma membrane through the exocytic pathway. *Mol Cell Biol* 2000; **20**: 2475–2487.
59 Faux MC, Rollins EN, Edwards AS, Langeberg LK, Newton AC, Scott JD. Mechanism of A-kinase-anchoring protein 79 (AKAP79) and protein kinase C interaction. *Biochem J* 1999; **343**(Pt 2): 443–452.
60 Gold MG, Stengel F, Nygren PJ, Weisbrod CR, Bruce JE, Robinson CV *et al.* Architecture and dynamics of an A-kinase anchoring protein 79 (AKAP79) signaling complex. *Proc Natl Acad Sci USA* 2011; **108**: 6426–6431.
61 Freye-Minks C, Kretsinger RH, Creutz CE. Structural and dynamic changes in human annexin VI induced by phosphorylation-mimicking mutation T356D. *Biochemistry* 2003; **42**: 620–630.
62 Minashima T, Small W, Moss SE, Kirsch T. Intracellular modulation of signaling pathways by Annexin A6 regulates terminal differentiation of chondrocytes. *J Biol Chem* 2012; **287**: 14803–14815.
63 Theobald J, Hanby A, Patel K, Moss SE, Annexin VI. has tumour-suppressor activity in human A431 squamous epithelial carcinoma cells. *Br J Cancer* 1995; **71**: 786–788.
64 Johannsdottir HK, Jonsson G, Johannesdottir G, Agnarsson BA, Eerola H, Arason A *et al.* Chromosome 5 imbalance mapping in breast tumors from BRCA1 and BRCA2 mutation carriers and sporadic breast tumors. *Int J Cancer* 2006; **119**: 1052–1060.
65 Pierga JY, Reis-Filho JS, Cleator SJ, Dexter T, Mackay A, Simpson P *et al.* Microarray-based comparative genomic hybridisation of breast cancer patients receiving neoadjuvant chemotherapy. *Br J Cancer* 2007; **96**: 341–351.
66 Boultwood J, Fidler C, Strickson AJ, Watkins F, Gama S, Kearney L *et al.* Narrowing and genomic annotation of the commonly deleted region of the 5q- syndrome. *Blood* 2002; **99**: 4638–4641.
67 Strzelecka-Kiliszek A, Buszewska ME, Podszywalow-Bartnicka P, Pikula S, Otulak K, Buchet R *et al.* Calcium- and pH-dependent localization of annexin A6 isoforms in

Balb/3T3 fibroblasts reflecting their potential participation in vesicular transport. *J Cell Biochem* 2008; **104**: 418–434.
68 Podszywalow-Bartnicka P, Kosiorek M, Piwocka K, Sikora E, Zablocki K, Pikula S. Role of annexin A6 isoforms in catecholamine secretion by PC12 cells: distinct influence on calcium response. *J Cell Biochem* 2010; **111**: 168–178.
69 Tonetti DA, Morrow M, Kidwai N, Gupta A, Badve S. Elevated protein kinase C alpha expression may be predictive of tamoxifen treatment failure. *Br J Cancer* 2003; **88**: 1400–1402.
70 Frankel LB, Lykkesfeldt AE, Hansen JB, Stenvang J. Protein Kinase C alpha is a marker for antiestrogen resistance and is involved in the growth of tamoxifen resistant human breast cancer cells. *Breast Cancer Res Treat* 2007; **104**: 165–179.
71 Assender JW, Gee JM, Lewis I, Ellis IO, Robertson JF, Nicholson RI. Protein kinase C isoform expression as a predictor of disease outcome on endocrine therapy in breast cancer. *J Clin Pathol* 2007; **60**: 1216–1221.
72 Timpson P, Wilson AS, Lehrbach GM, Sutherland RL, Musgrove EA, Daly RJ. Aberrant expression of cortactin in head and neck squamous cell carcinoma cells is associated with enhanced cell proliferation and resistance to the epidermal growth factor inhibitor gefitinib. *Cancer Res* 2007; **67**: 9304–9314.
73 Jaumot M, Hancock JF. Protein phosphatases 1 and 2A promote Raf-1 activation by regulating 14-3-3 interactions. *Oncogene* 2001; **20**: 3949–3958.
74 Lladó A, Timpson P, Vilà de Muga S, Moretó J, Pol A, Grewal T *et al.* PKCδ and calmodulin regulate recycling from the early endosomes through Arp2/3 and cortactin. *Mol Biol Cell* 2008; **19**: 17–29.

Supplementary Information accompanies the paper on the Oncogene website (http://www.nature.com/onc)